



## AN ABSTRACT OF THE THESIS OF

Brett Peterson for the degree of Master of Science in  
Electrical and Computer Engineering presented on February 20, 2008.

Title: Automated Model Parameter Extraction for  
Noise Coupling Analysis in Silicon Substrates

Abstract approved:

---

Terri S. Fiez

Karti Mayaram

An automated method, requiring the fabrication of a small set of test structures, efficiently extracts the coefficients of Z-parameter based macromodels. The extraction approach has been validated for both heavily and lightly doped substrates and can be applied to a variety of technologies. After the parameters of a macromodel have been extracted, the model can be used to quickly and accurately calculate the equivalent substrate network connecting an arbitrary number of contacts. This automated extraction process has been integrated into the Cadence DFII environment to provide a seamless flow for substrate noise analysis.

©Copyright by Brett Peterson  
February 20, 2008  
All Rights Reserved

Automated Model Parameter Extraction for Noise Coupling  
Analysis in Silicon Substrates

by

Brett Peterson

A THESIS

submitted to

Oregon State University

in partial fulfillment of  
the requirements for the  
degree of

Master of Science

Presented February 20, 2008

Commencement June 2008

Master of Science thesis of Brett Peterson presented on February 20, 2008.

APPROVED:

---

Co-Major Professor, representing Electrical and Computer Engineering

---

Co-Major Professor, representing Electrical and Computer Engineering

---

Director of the School of Electrical Engineering and Computer Science

---

Dean of the Graduate School

I understand that my thesis will become part of the permanent collection of Oregon State University libraries. My signature below authorizes release of my thesis to any reader upon request.

---

Brett Peterson, Author

## ACKNOWLEDGEMENTS

I would first like to thank my advisers, Dr. Terri Fiez and Dr. Kartikeya Mayaram, whose guidance and support was indispensable throughout my graduate education. I am truly grateful for the opportunities they have given me. I would also like to thank my GCR, Nathan Gibson, for his consultation on the content in Chapter 3. Additionally, I thank Defense Advanced Research Projects Agency (DARPA) and Semiconductor Research Corporation (SRC) for funding my research.

During my time at Oregon State University I have come to know many outstanding individuals. I am fortunate to have been a part of the substrate coupling group and work alongside Matt MacClary, Chris Hanken, Jim Le, Arthi Sundaresan, Kavitha Srinivasan, Andrew Tabalujan, Robert Shreeve, Wailang Cheong, and Jacky Wong. All of these people helped to create an enjoyable and collaborative learning environment. I would like to thank Lou Hu, Napong Panitantum, Peter Kurahashi, Dave Gubbins, James Ayers, and Robert Batten for all of the help they have provided me during my studies and research.

I would never have made it this far without a little help from my friends. I want to thank Dustin Way, Andrew Northy, Brian Lilley, Matt Rodger, and Matt Gould for all of the experiences they have shared with me over the years.

Finally, I would like to thank my parents, Char and Craig, and my brother,

Trevor, who constantly inspire me to do my best. Their unyielding love and support has given me the strength to accomplish more than I ever thought I was capable of.

# TABLE OF CONTENTS

	<u>Page</u>
1 Introduction	1
1.1 Background and Motivation . . . . .	1
1.2 Thesis Outline . . . . .	3
2 Existing Substrate Modeling Methods	4
2.1 Heavily and Lightly Doped Substrates . . . . .	4
2.2 Numerical Techniques for Substrate Network Extraction . . . . .	5
2.3 Macromodels For Substrate Network Calculation . . . . .	6
2.4 Resistive Substrate Coupling Model . . . . .	6
2.5 Substrate Macromodels . . . . .	7
2.5.1 Models for Heavily Doped Substrates . . . . .	8
2.5.2 Model for Lightly Doped Substrates . . . . .	9
2.5.3 Implementing Macromodels in New Technologies . . . . .	10
3 Automated Macromodel Parameter Extraction	11
3.1 High Level Flow . . . . .	11
3.2 Calibration of the Substrate Doping Profile . . . . .	14
3.2.1 The Calibration Process . . . . .	14
3.2.2 Contact Selection for Input Measurements . . . . .	15
3.2.3 Limitations of the Calibration Method . . . . .	19
3.2.4 Constrained Calibration . . . . .	20
3.2.5 Simplified Calibration . . . . .	23
3.3 Generating the $Z_{12}$ Dataset . . . . .	29
3.4 Model Parameter Extraction . . . . .	31
3.5 Implementation in Cadence . . . . .	33
4 Measurements and Validation	36
4.1 Measurements . . . . .	36
4.2 Validating the Calibration . . . . .	38
4.3 Validating the Parameter Extraction Procedure . . . . .	40

## TABLE OF CONTENTS (Continued)

	<u>Page</u>
5 Silencer! and Assura Substrate Extraction	49
5.1 Comparing Silencer! and Assura RCX . . . . .	49
5.1.1 Parasitic and Substrate Extraction . . . . .	50
5.1.2 Transient Simulations . . . . .	52
5.1.3 User Experience . . . . .	54
6 Conclusion	58
Bibliography	60
Appendices	63
A Contact Pairs Used for Dataset Generation . . . . .	64
B Implementing a New Macromodel . . . . .	66
C Model Parameter Extraction With Silencer! . . . . .	69
D Modifications to the Calibration Routine . . . . .	85

## LIST OF FIGURES

Figure	Page
1.1 Substrate noise coupling in mixed-signal ICs. . . . .	2
2.1 Layered approximations of a heavily doped (left) and lightly doped (right) silicon substrate. . . . .	5
2.2 Resistive substrate model. . . . .	7
2.3 Geometric parameters used in the $Z_{12}$ model equations. . . . .	9
3.1 Input-output relationship for automated model parameter extraction.	12
3.2 Automated model parameter extraction flow. . . . .	13
3.3 Calibration of a heavily doped substrate. . . . .	15
3.4 Approximate current spreading for various contact sizes. . . . .	17
3.5 Calibrated doping profiles from four different sets of initial conditions.	21
3.6 Doping profile after a constrained calibration. The final values of the channel stop and epi thickness are: $t_{ch} = 0.4\mu\text{m}$ and $t_{epi} = 4.6\mu\text{m}$ .	23
3.7 Doping profiles after calibrating with constraints on only the channel stop thickness ( $0.2\mu\text{m} \leq t_{ch} \leq 0.5\mu\text{m}$ ) and only the epi thickness ( $3.5\mu\text{m} \leq t_{epi} \leq 5\mu\text{m}$ ). For the case where $t_{epi}$ is constrained, the final values of the channel stop and epi thickness are: $t_{ch} = 0.41\mu\text{m}$ and $t_{epi} = 3.57\mu\text{m}$ . For the case where $t_{ch}$ is constrained, the final values of the channel stop and epi thickness are: $t_{ch} = 0.5\mu\text{m}$ and $t_{epi} = 7.8\mu\text{m}$ . . . . .	24
3.8 Sum of squared errors in the heavily doped substrate with constant channel stop parameters. An inverse relationship can be observed between the epi thickness and resistivity. . . . .	26
3.9 Sum of squared errors in the heavily doped substrate with constant epi layer parameters. A linear relationship can be observed between the channel thickness and resistivity. . . . .	27
3.10 The resistivity and thickness values of the channel stop layer for four different calibrated profiles shows that a linear relationship exists for practical ranges of these parameters. . . . .	28

## LIST OF FIGURES (Continued)

Figure	Page
3.11 Calibration with the epi thickness fixed at $4.5\mu\text{m}$ . . . . .	30
3.12 Dataset generation and model parameter extraction using a calibrated doping profile and a large variety of contact configurations. . .	32
3.13 Extracting model parameters with a curve-fitting procedure. . . . .	33
3.14 Graphical user interface for setting up the automated parameter extraction. . . . .	35
4.1 Die photo of the test chip fabricated in a $0.35\mu\text{m}$ CMOS process. . .	37
4.2 Die photo of the test chip fabricated in a $0.25\mu\text{m}$ CMOS process. . .	37
4.3 Measurement setup for the direct measurement of Z-parameters. . . .	38
4.4 Results from the calibration of each substrate. . . . .	41
4.5 A comparison of measurements with EPIC simulations before (EPIC-Pre) and after (EPIC-Post) calibration for the $0.35\mu\text{m}$ heavily doped substrate. . . . .	42
4.6 A comparison of measurements with EPIC simulations before (EPIC-Pre) and after (EPIC-Post) calibration for the $0.25\mu\text{m}$ heavily doped substrate. . . . .	42
4.7 A comparison of measurements with EPIC simulations before (EPIC-Pre) and after (EPIC-Post) calibration for the lightly doped substrate. . . . .	43
4.8 Relative error in $Z_{12}$ versus contact separation for the heavily doped macromodel (2.1) (top) and (2.3) (bottom) after parameter extraction. Errors in these plots are reported with respect to EPIC simulations in the $0.35\mu\text{m}$ process. Each curve represents the error for a different pair of contacts. . . . .	44
4.9 Relative error in $Z_{12}$ versus contact separation for the heavily doped (top) and lightly doped (bottom) macromodels after parameter extraction. Errors in these plots are reported with respect to EPIC simulations in the $0.25\mu\text{m}$ process. Each curve represents the error for a different pair of contacts. . . . .	46

## LIST OF FIGURES (Continued)

<u>Figure</u>		<u>Page</u>
4.10	A comparison between measurements and the macromodel after extraction for the $0.35\mu\text{m}$ heavily doped process. . . . .	47
4.11	A comparison between measurements and the macromodel after extraction for the $0.25\mu\text{m}$ heavily doped process. . . . .	48
4.12	A comparison between measurements and the macromodel after extraction for the $0.25\mu\text{m}$ lightly doped process. . . . .	48
5.1	The extraction processes for Silencer! and Assura RCX and a comparison of the number of extracted elements. Assura extracts more elements for its substrate network because it uses a more complicated model. . . . .	51
5.2	Simulated transient waveforms at the output of the op-amp with substrate networks from Assura RCX and Silencer! are compared with measurements. . . . .	53
5.3	Simulated transient waveforms at the output of the op-amp without the extracted substrate network. All of the coupling in this case is a result of the mutual inductance of the bondwires. . . . .	55
5.4	Simulated transient waveforms at the output of the op-amp with the extracted substrate network and no parasitic capacitances. . . .	56

## LIST OF TABLES

<u>Table</u>		<u>Page</u>
3.1	Current spreading for contacts in the $0.25\mu\text{m}$ heavily doped substrate.	17
3.2	Scalable contact set for calibrating heavily and lightly doped processes. $\lambda$ is the minimum side length of a substrate contact. . . . .	19
4.1	Contact list for calibrating each substrate doping profile. . . . .	39
5.1	A comparison of Silencer! and Assura RCX based on the design used in this chapter. . . . .	57

## LIST OF APPENDIX FIGURES

<u>Figure</u>		<u>Page</u>
B.1	The interface between the parameter extraction code and the shared object. . . . .	67

## LIST OF APPENDIX TABLES

<u>Table</u>		<u>Page</u>
A.1	Contact pairs used to simulate $Z_{12}$ values for the dataset from which model parameters are extracted. . . . .	65

## Chapter 1 – Introduction

### 1.1 Background and Motivation

The continued scaling of technology has motivated the need to integrate analog, radio frequency (RF), and digital circuitry onto a single silicon substrate. The result is the development of complex Systems-on-a-Chip (SoC) which possess many advantages including reduced size and cost as well as increased performance. There are, however, undesirable characteristics which accompany the increased complexity and integration. Many circuits, all with different functions, now operate in close proximity on a shared substrate and unintended interactions are inevitable.

When analog and digital blocks are placed on the same silicon substrate, substrate coupling may become a serious issue. Digital blocks inject noise into the substrate through the gate capacitance or the drain junction capacitance at signal transitions. The switching noise then propagates throughout the substrate and can perturb the sensitive analog circuitry through the body effect and capacitive coupling between the substrate and the gate, drain, and source nodes [1]. Fig. 1.1 provides a visualization of the substrate coupling mechanism. Many factors including the physical separation between the analog and digital circuits as well as the substrate doping levels determine the severity of the noise coupling. Substrate noise coupling is a growing problem and will continue to compromise the perfor-

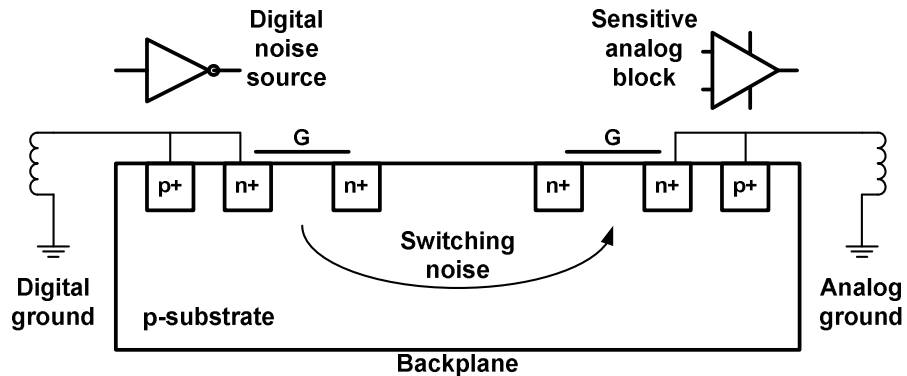


Figure 1.1: Substrate noise coupling in mixed-signal ICs.

mance of modern SoC designs if the proper measures are not taken to mitigate its effects.

Various methods for modeling substrate coupling have been developed in recent years. Many of these techniques involve numerical simulations [2-8] which yield accurate results but are time consuming even for small circuits. Numerical solutions also require a completed chip layout which forces designers to go through complete design iterations in order to minimize noise coupling. Other solutions use macromodels to calculate the substrate network [9-14] or hybrid approaches such as polynomial curve-fitting [15] which use a combination of numerical and macromodel based techniques. Macromodel based approaches are orders of magnitude faster than numerical techniques because they directly evaluate mathematical expressions. Pre-layout analysis is also enabled by using macromodels. These qualities make macromodels the best choice for simulating substrate coupling in large SoC designs. However, macromodels are inherently process specific because they contain many process related parameters. So, for the efficient analysis of

substrate coupling, a method is needed which allows the model parameters to be easily obtained. This thesis presents an automated process for the extraction of model parameters for substrate noise coupling analysis in silicon substrates.

## 1.2 Thesis Outline

The thesis is organized as follows: Chapter 2 gives a brief overview of previous work in substrate modeling. The methodology for automated model parameter extraction as well as a discussion of each functional block in the extraction flow is presented in Chapter 3. Chapter 4 provides a step by step validation of the parameter extraction process, proving the effectiveness of the critical functions. A comparison of two substrate noise simulation tools is given in Chapter 5. Finally, Chapter 6 concludes the thesis and explores some possibilities for future work.

## Chapter 2 – Existing Substrate Modeling Methods

As stated previously, many techniques have been developed that address the issue of substrate modeling. This chapter begins with a brief overview of heavily and lightly doped substrates followed by a discussion of a few existing techniques for substrate network extraction. The final portion of this chapter investigates a resistive model for the substrate coupling network and the macromodels that are used in this work.

### 2.1 Heavily and Lightly Doped Substrates

Silicon substrates can be divided into two broad categories: heavily doped substrates and lightly doped substrates. The two types of substrates are characterized by their doping profiles, which can be approximated by discrete layers of uniform resistivity as seen in Fig. 2.1. Lightly doped substrates are composed of a thin, low-resistivity channel-stop layer on top of a highly resistive bulk. Heavily doped substrates have a low-resistivity channel-stop layer and a low-resistivity bulk which are separated by a high-resistivity epitaxial layer which reduces latch-up problems.

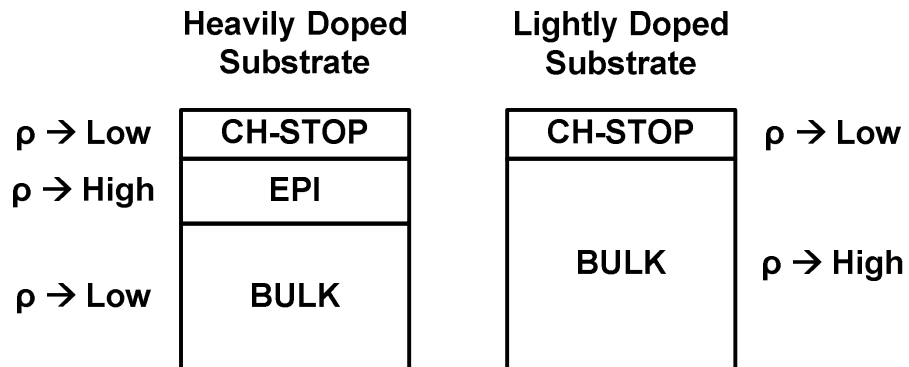


Figure 2.1: Layered approximations of a heavily doped (left) and lightly doped (right) silicon substrate.

## 2.2 Numerical Techniques for Substrate Network Extraction

Several numerical methods can be used to accurately characterize silicon substrates. These methods can be broken down into two broad categories which include volume element methods and boundary element methods.

The finite element method (FEM) and finite difference method (FDM), used to numerically solve partial differential equations, are powerful and versatile tools which can be employed to model silicon substrates. To utilize this method, the entire volume of the substrate and the contacts under consideration are divided into a mesh and Poisson's equation is solved to find the potential variation [2]. This method is highly accurate but the full discretization of the substrate leads to very large matrices and long simulation times which compound as the design size increases. Boundary element methods (BEM) perform a similar function but are generally preferred to the FEM/FDM because they are computationally more efficient and also yield accurate simulation results [4, 5]. Although the FEM/FDM

and BEM provide a high degree of accuracy, they are not appropriate for pre-layout noise estimation and are applicable only for small circuits.

### 2.3 Macromodels For Substrate Network Calculation

Macromodels provide designers with an additional method to simplify substrate coupling. In practice, macromodel based approaches are less accurate than numerical methods but offer many crucial advantages. These models are obtained by curve-fitting simulated or measured data and are used to directly calculate substrate impedances or resistances. Some benefits of using macromodels, which were mentioned earlier, include short simulation times and the capability of pre-layout analysis. Scalable macromodels, which calculate a substrate network based on the geometry and separation of the contacts, greatly reduce the complexity of substrate extraction. Macromodels are not general solutions, however, and must be adapted to each new process. This is because macromodels contain many process specific coefficients whose values are determined by curve fitting and are unique for a given process.

### 2.4 Resistive Substrate Coupling Model

For frequencies below a few GHz, both the heavily doped and lightly doped substrates can be modeled by a purely resistive network [16]. In a simple, two contact case, the equivalent substrate network is modeled by a  $\pi$  resistor network shown in

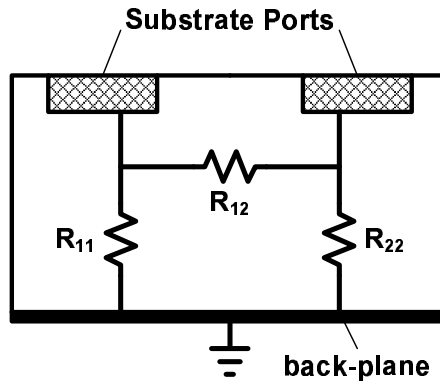


Figure 2.2: Resistive substrate model.

Fig. 2.2. It is an easy task to include the resistive network into circuit simulations. However, using macromodels directly for calculating the substrate resistances can cause problems for analyzing multiport situations [9]. For this reason, the substrate is typically modeled with open circuit impedance parameters and, thus, macromodels are developed which evaluate the  $Z$ -parameters for a pair of contacts. The resistive substrate network can be easily calculated from the  $Z$ -parameters and included in a schematic for noise coupling simulations.

## 2.5 Substrate Macromodels

Three different  $Z$ -parameter based macromodels are used in this work. Two macromodels have been developed for heavily doped substrates [9, 10] and another for lightly doped substrates [11]. In both cases, the macromodels contain explicit mathematical expressions for the  $Z$ -parameters for two substrate contacts. This work focuses primarily on the model for  $Z_{12}$  because it is more complex than the

model for  $Z_{11}$ . This is due to the fact that the  $Z_{11}$  model does not depend on the separation between the two contacts in any of these models.

### 2.5.1 Models for Heavily Doped Substrates

The  $Z_{12}$  models for heavily doped substrates are functions of the separation between the two contacts as well as contact geometry. The first macromodel equation is scalable with contact area and perimeter [9].

$$Z_{12} = \alpha e^{\beta x} \quad (2.1)$$

The separation between the contacts is given by  $x$  and the value for  $\alpha$  is calculated when the separation between the two contacts is zero and the contacts are merged.

$$\alpha = \frac{1}{K_1 A_t + K_2 P_t + K_3} \quad (2.2)$$

where  $A_t$  is the total area of the merged contact,  $P_t$  is the perimeter of the merged contact and  $K_1$ ,  $K_2$ , and  $K_3$  are process related constants.  $\beta$  is also a process related constant.

The second macromodel for heavily doped substrates takes on a similar form but is more complicated and achieves a much higher level of accuracy [10].

$$Z_{12} = \alpha e^{\beta x^{0.75}} \quad (2.3)$$

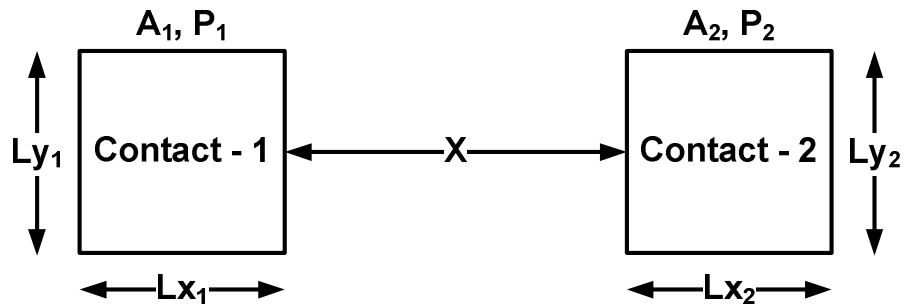


Figure 2.3: Geometric parameters used in the  $Z_{12}$  model equations.

where  $\alpha$  is given by

$$\alpha = \frac{1}{c_1(Lx_1 + Lx_2)^{c_2} + c_3(Ly_1 + Ly_2)^{c_4} + c_5(Lx_1 + Lx_2)(Ly_1 + Ly_2) + c_6} \quad (2.4)$$

and  $\beta$  is given by

$$\beta = \frac{1}{c_7(P_1 + P_2) + c_8} \quad (2.5)$$

where  $x$  is the separation between the two contacts,  $c_1 - c_8$  represent process related constants,  $Lx_1$  and  $Ly_1$  are the x- and y-dimensions of the first contact,  $Lx_2$  and  $Ly_2$  are the x- and y-dimensions of the second contact, and  $P_1$  and  $P_2$  are the perimeters of the first and second contact, respectively. The geometric parameters can be visualized as shown in Fig. 2.3.

## 2.5.2 Model for Lightly Doped Substrates

The  $Z_{12}$  model for lightly doped substrates is a function of contact geometry and the geometric mean distance (GMD). The GMD is a parameter which can si-

multaneously account for the separation between the substrate contacts and their geometry [17]. This results in a much more compact equation for  $Z_{12}$  [11].

$$Z_{12} = [k_1(W_1 + W_2) + k_2]e^{-k_3\sqrt{GMD}} \quad (2.6)$$

where  $k_1 - k_3$  are process related constants and  $W_1$  and  $W_2$  are the widths of the two contacts.

### 2.5.3 Implementing Macromodels in New Technologies

All of the  $Z_{12}$  models discussed in this chapter contain a set of process related constants which is unique for each and every technology. As mentioned earlier in this chapter, the process related constants must be extracted before the model can be used for a given technology. The task of extracting these constants typically requires a curve-fitting operation which relies on a large set of measured or simulated data as a reference. In the following chapter, a method is presented which automates the accurate extraction of these parameters allowing macromodels to be easily adapted to any technology.

## Chapter 3 – Automated Macromodel Parameter Extraction

In this chapter, an automated technique for the extraction of model parameters is presented. An overview of the parameter extraction flow is then given, followed by a detailed description of each of the functional blocks. Finally, the implementation of the parameter extraction flow within the Cadence DFII environment is discussed.

### 3.1 High Level Flow

The automated model parameter extraction, which is developed in this section, is based on a simple input-output relationship shown in Fig. 3.1. The required input data includes a small set of  $Z_{11}$  measurements, an estimate of the substrate doping profile, and the macromodel equations. The output contains the extracted model parameters for the input macromodel equations, allowing the macromodel to accurately calculate substrate parameters.

It is typical to use a curve-fitting approach to extract the parameters for a mathematical model and this approach is taken here. To produce optimal results with the curve-fitting procedure, a large set of reference values must be used. This reference set contains data for a sample of contact configurations, varied in size, shape, and separation, which covers all of the scenarios for which the macromodel is valid. Either simulated or measured data can be used to populate the reference

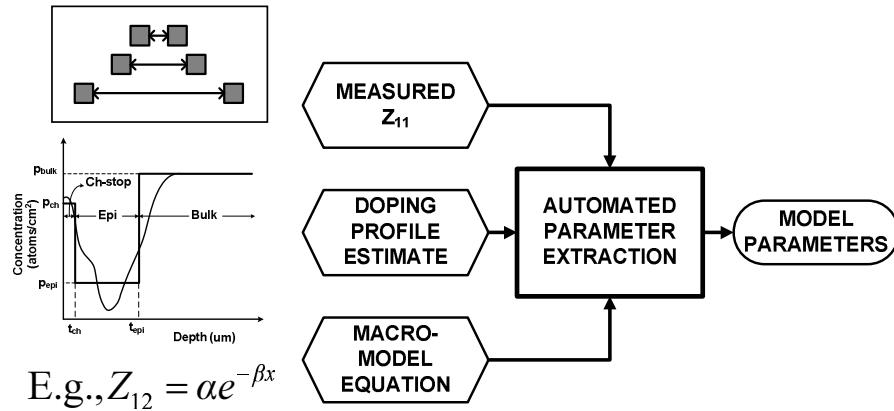


Figure 3.1: Input-output relationship for automated model parameter extraction.

dataset. Using measured data would require the fabrication of many test structures and obtaining measurements is much more expensive and time consuming than performing simulations. For these reasons, use of a numerical simulator for generating a large reference set is a much better option. However, accurately simulating substrate parameters requires a precise knowledge of the substrate doping levels. Because the doping information is not typically available, some means of obtaining an approximation of the substrate doping profile is needed.

EPIC, a 3-dimensional Green's function solver [18], is utilized for numerical simulations in this work. The input to EPIC is a layered approximation of the substrate doping profile, simulation options, and a description of the contact configurations. In order to match EPIC simulations with measurements, the layered doping profile approximation must be accurate. The calibration procedure presented in [19], which is discussed in detail in the next section, is used to generate the layered approximation. Once the substrate doping profile is calibrated, EPIC simulations are used to generate a large reference set from which the macromodel

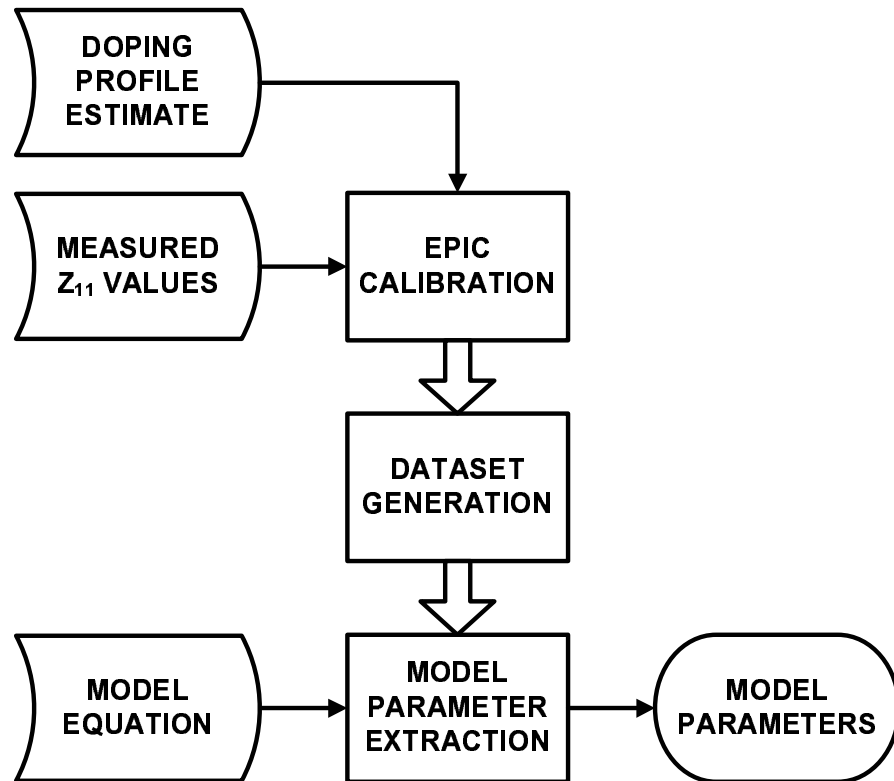


Figure 3.2: Automated model parameter extraction flow.

parameters can be extracted. A block diagram that represents the entire parameter extraction process is shown in Fig. 3.2. The first two steps in this figure utilize numerical simulations performed by EPIC to first calibrate the substrate doping profile and then generate a dataset of  $Z$ -parameters. The last step is to extract the parameters of the model equation based on the simulated dataset. Finally, with the extracted model parameters, a SPICE-like simulator can be used to simulate substrate noise coupling in complex mixed-signal SoCs.

## 3.2 Calibration of the Substrate Doping Profile

The first step in the model parameter extraction flow is calibration of the substrate doping profile. In this step, the substrate profile is characterized so that accurate numerical simulations can be performed. The following paragraphs discuss the calibration procedure in more detail as well as modifications made to improve performance and increase the accuracy of the calibrated profile.

### 3.2.1 The Calibration Process

The substrate doping profile is calibrated by making comparisons between measured and simulated data in an optimization loop. The error information is used to adjust the doping profile in order to make the simulations match the measurements. This process is illustrated in Fig. 3.3. The minimization of the error is driven by a Levenberg-Marquardt Algorithm (LMA), which is often used in least squares curve-fitting problems and nonlinear function minimization [20].

To calibrate a profile for EPIC, DC  $Z_{11}$  measurements for isolated contacts are compared with results from the corresponding EPIC simulations. An initial estimate of the substrate doping profile is also required. This estimate serves as a starting point from which the LMA can begin to minimize the error in simulation. This is accomplished by changing the thickness and resistivity of the layers in the input doping profile for EPIC according to calculations which are based on the error information [19]. When the calibration is done, the layered profile is optimized so that EPIC simulations match the measured  $Z_{11}$  values. Then, EPIC can be used

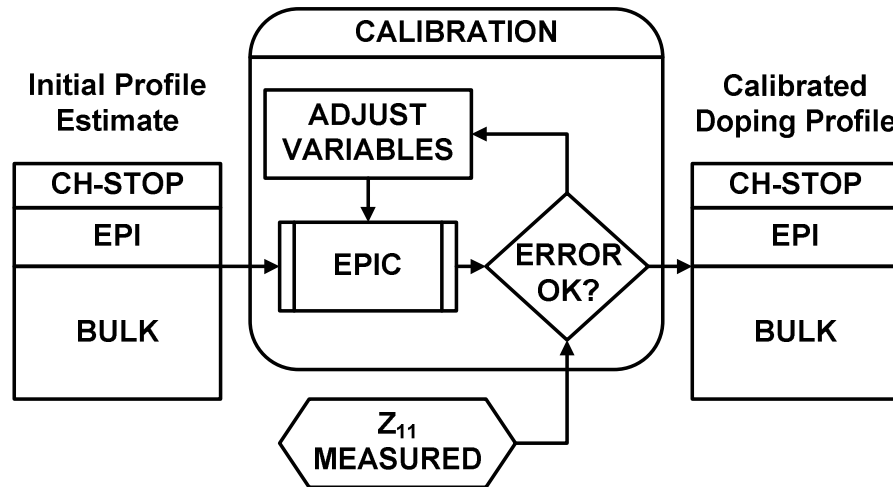


Figure 3.3: Calibration of a heavily doped substrate.

to accurately calculate  $Z_{11}$  and  $Z_{12}$  values. Thus, a set of valid reference data can be created for the macromodel parameter extraction.

### 3.2.2 Contact Selection for Input Measurements

A fundamental part of calibration is the selection of contacts for  $Z_{11}$  measurements and simulations. To understand why contact selection is so important, an explanation of the physical characteristics of the substrate contacts is required. This discussion will be focused primarily on the heavily doped substrate.

It is important to note that the resistance of the epi layer will dominate the total resistance between a contact and the backplane. Also, the resistance from an isolated contact to the backplane is nearly equal to the  $Z_{11}$  value for the contact. So, to calculate the approximate value for a contact's self resistance and, thus, the

approximate  $Z_{11}$  value for the contact, one can simply use the equation

$$R = \frac{\rho t}{A} \quad (3.1)$$

where  $\rho$  is the resistivity of the epi layer,  $t$  is the thickness of the epi layer, and  $A$  is the area of the substrate contact. This calculation assumes that all of the current flows vertically from the contact to the backplane. This is an invalid assumption because there is current spreading in the low-resistivity channel stop layer.

As a result of current spreading, any given contact will have an effective area which is larger than the physical area of the contact. It can be observed from  $Z_{11}$  measurements that the current will spread by a relatively constant amount as shown in Fig. 3.4. In the case of the  $0.25\mu\text{m}$  heavily doped process, the current spreads approximately  $10\mu\text{m}$  from the side of a contact. For contacts smaller than about  $2\mu\text{m} \times 2\mu\text{m}$ , the effective area is many times larger than the area of the contact itself. For contacts larger than about  $100\mu\text{m} \times 100\mu\text{m}$ , the spreading distance will actually decrease slightly and the contact area will become very close in value to the effective area. In Table 3.1,  $Z_{11}$  values are simulated for various contacts and values for the spreading distance are calculated based on the difference between the effective contact area and the physical contact area.

The physical characteristics of substrate contacts that were just discussed must be kept in mind during contact selection for the calibration procedure. There are two factors at work which control  $Z_{11}$ . These are the resistivity-thickness product of the epi layer and the spreading in the channel stop layer. The value of  $Z_{11}$  for

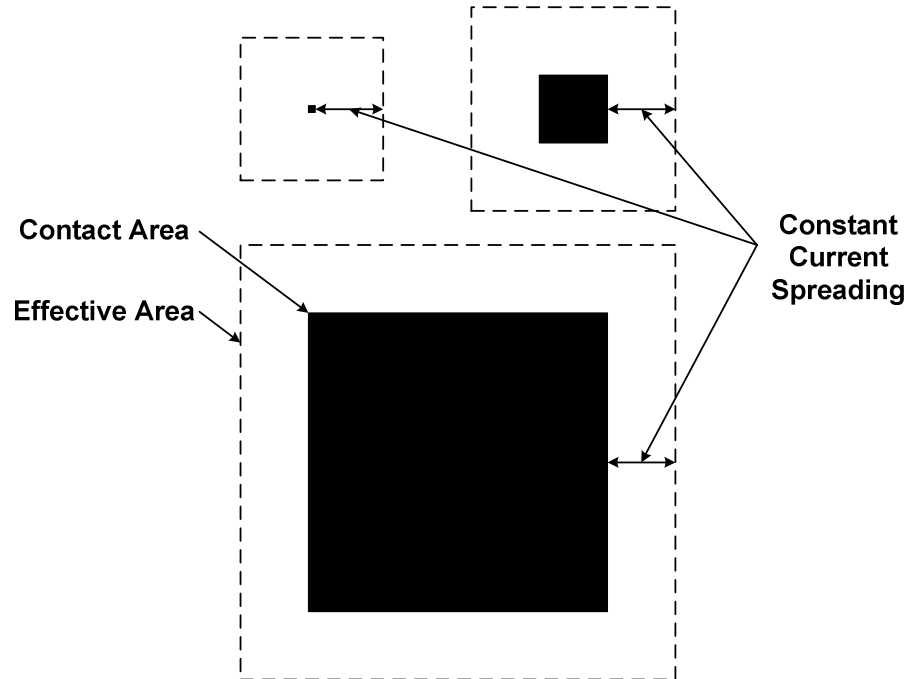


Figure 3.4: Approximate current spreading for various contact sizes.

Table 3.1: Current spreading for contacts in the  $0.25\mu\text{m}$  heavily doped substrate.

Contact Size	$Z_{11}(\Omega)$	Spreading ( $\mu\text{m}$ )
$1\mu\text{m} \times 1\mu\text{m}$	1340	8.7
$2\mu\text{m} \times 2\mu\text{m}$	1007	9.6
$5\mu\text{m} \times 5\mu\text{m}$	655	10.6
$10\mu\text{m} \times 10\mu\text{m}$	428	11.2
$20\mu\text{m} \times 20\mu\text{m}$	244	11.5
$50\mu\text{m} \times 50\mu\text{m}$	87.5	10.9
$100\mu\text{m} \times 100\mu\text{m}$	32.5	8.8
$200\mu\text{m} \times 200\mu\text{m}$	10.4	4.0

very large contacts is not dependent on the spreading because the contact area is nearly equal to the effective area. This means that variations in the channel stop will not significantly affect  $Z_{11}$  value for large contacts. It would be possible to independently extract the resistivity-thickness product of the epi layer by using very large contacts ( $300\mu\text{m} \times 300\mu\text{m}$  or larger). However, this is not always practical because of the area requirements. Contacts with sizes around the  $50\mu\text{m}$  or  $100\mu\text{m}$  range will still be useful for extracting the epi layer parameters. Smaller contacts will allow the extraction of the channel stop parameters because the  $Z_{11}$  values are much more dependent on the spreading. For the heavily doped  $0.25\mu\text{m}$  technology, it is practical to use a distribution of contacts between  $0.25\mu\text{m} \times 0.25\mu\text{m}$  and  $50\mu\text{m} \times 50\mu\text{m}$ . Using such a contact set for input  $Z_{11}$  measurements allows the channel stop and epi layer parameters to be accurately extracted during calibration. Lightly doped substrates only need to have their channel stop region calibrated but spreading is much more significant in lightly doped substrates. Using contacts with a range of sizes similar to those used for the heavily doped substrate will increase the range of  $Z_{11}$  values and allow the channel stop parameters to be extracted accurately. In fact, the same contact set can be used to successfully calibrate both heavily and lightly doped substrates. Table 3.2 contains a generic contact set, based on the minimum square contact size, which can be scaled to a variety of technologies. Rectangular contacts can be used instead of square contacts, however, square contacts provide the best ratio of contact area to effective area.

Table 3.2: Scalable contact set for calibrating heavily and lightly doped processes.  $\lambda$  is the minimum side length of a substrate contact.

Contact Size
$\lambda \times \lambda$
$5\lambda \times 5\lambda$
$20\lambda \times 20\lambda$
$50\lambda \times 50\lambda$
$100\lambda \times 100\lambda$
$200\lambda \times 200\lambda$

### 3.2.3 Limitations of the Calibration Method

The success of the calibration approach can be quantified by how well the simulated Z-parameters agree with measurements. Another important consideration is simulation time. Because numerical simulations are being performed in a loop, calibration can be a lengthy procedure. There are several factors related to the input data which can affect the results and the time required for calibration. These include the number of layers used to approximate the substrate, the initial profile estimate, and the choice and accuracy of input measurements. It has been shown in [19] that a 3-layer profile for heavily doped substrates provides sufficient accuracy while keeping the simulation time as low as possible. Similarly, a 2-layer profile can be used for lightly doped substrates to achieve a good degree of accuracy. Another factor is the doping profile estimate, which is meant to provide a starting point for the calibration. Less accuracy in the estimate means that the LMA will take longer to converge and the simulation time will increase. As described in the previous section, using a range of contact sizes for the input is important in order to narrow the solution space. If all of the contacts are similar in size, then the

range of  $Z_{11}$  values is small. This can cause the calibration to converge improperly and generate an inaccurate doping profile. Similar problems arise if there are any inconsistent measurements.

The accuracy of the initial profile estimate, in part, determines the accuracy of the output profile. Because it is a starting point for the profile calibration, variations in the estimate will cause the output profile to evolve differently. This variation can be seen in Fig. 3.5. To create this plot, different initial conditions were used for each calibration and the result is a wide array of output profiles. Each set of initial conditions that was used is actually closer to the expected profile than the calibrated results. The expected profile is determined from the spreading resistance profile (SRP) data. These profiles all predict  $Z_{11}$  accurately because there are many possible combinations of the channel stop and epi layer parameters that result in the same  $Z_{11}$  values. However, none of these profiles are good representations of the substrate. Because of the sensitivity to the initial conditions, it is critical to provide a highly accurate doping profile estimate in order to obtain an accurate calibrated profile. This is a shortcoming of the existing implementation of the calibration method. Techniques to overcome these limitations are presented in the following sections.

### 3.2.4 Constrained Calibration

One way to prevent the output profile from having unreasonable thickness and resistivity values is to enforce constraints on these parameters. To test this ap-

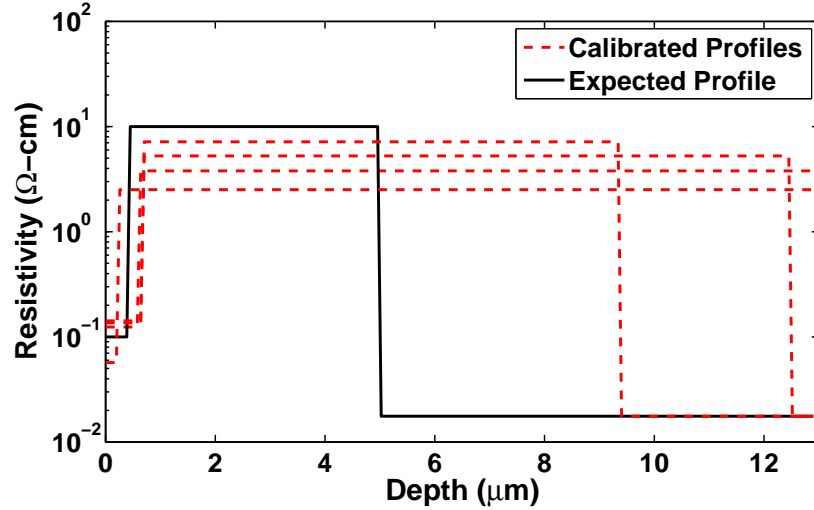


Figure 3.5: Calibrated doping profiles from four different sets of initial conditions.

proach, the calibration method was modified to allow the user to assign an upper and lower bound for the thickness of each layer in the substrate profile.

$$t_{ch\_min} \leq t_{ch} \leq t_{ch\_max} \quad (3.2)$$

$$t_{epi\_min} \leq t_{epi} \leq t_{epi\_max} \quad (3.3)$$

In these relationships,  $t_{ch}$  and  $t_{epi}$  which are the channel and epi layer thicknesses, respectively, must stay within a range specified by the user.  $t_{ch\_min}$  and  $t_{ch\_max}$  are the minimum and maximum values for the thickness of the channel stop layer.  $t_{epi\_min}$  and  $t_{epi\_max}$  are the minimum and maximum values for the thickness of the epi layer. If, at any time during the calibration, a profile has thickness values

outside the given constraints, the  $Z_{11}$  value from simulation is adjusted by a cost function which forces the error to be large. This prevents the calibration procedure from generating profiles with thicknesses that are too large or small. Also, because the resistance to the backplane is determined by the product of the resistivity and thickness of each layer, the constraint on the thickness of each layer will intrinsically provide a constraint on the resistivity of each layer.

A calibration with constraints on the layer thicknesses has been performed using one of the sets of initial conditions that generated an inaccurate doping profile from Fig. 3.5. In this calibration, the thickness of the channel stop layer is constrained between  $0.2\mu\text{m}$  and  $0.5\mu\text{m}$  and the thickness of the epi layer is constrained between  $3.5\mu\text{m}$  and  $5\mu\text{m}$ . The results can be observed in Fig. 3.6 and show that the constrained calibration offers a significant improvement over the unconstrained version.

To simplify the constrained calibration, it is possible to limit the number of constraints so that only one of the layers is bound to a user defined range. This will work based on the fact that the  $Z_{11}$  value for a contact is not dependent on individual contributions from the channel stop and epi layers, but rather on a combination of their properties. Thus, constraining the thickness of one layer will indirectly constrain the parameters of the other layer. Plots of the profiles calibrated with a single constraint are shown in Fig. 3.7. These calibrated profiles are less accurate than the profiles calibrated with constraints on both the channel stop and epi layer thickness. However, these profiles are still more accurate than those generated by the unconstrained calibration. While it is better to constrain

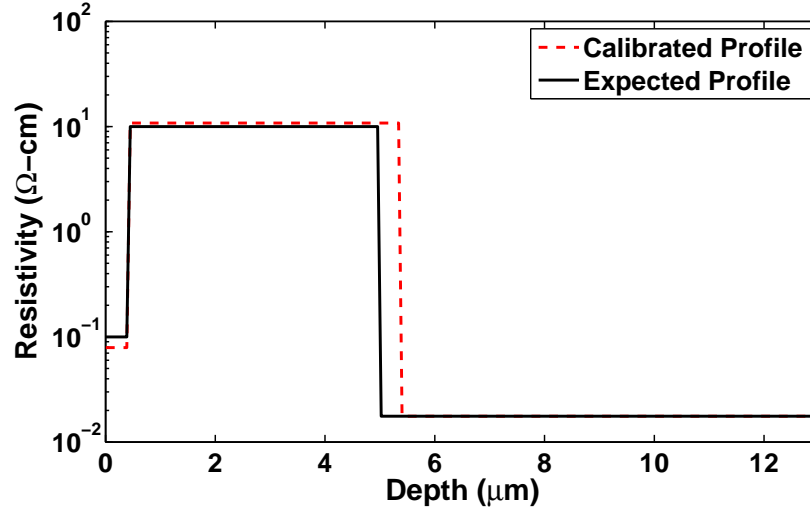


Figure 3.6: Doping profile after a constrained calibration. The final values of the channel stop and epi thickness are:  $t_{ch} = 0.4\mu\text{m}$  and  $t_{epi} = 4.6\mu\text{m}$ .

both the channel stop and epi layer, constraining one or the other will still provide reasonably accurate results.

An important observation is that the final thickness values after a constrained calibration, especially when only one parameter is constrained, always approach one of the limits of the constraint. While this method can still be used to generate accurate profiles, a more practical approach is discussed in the following section.

### 3.2.5 Simplified Calibration

As stated previously, many possible substrate profiles exist which can yield accurate simulation results. While some of these solutions do not precisely match the

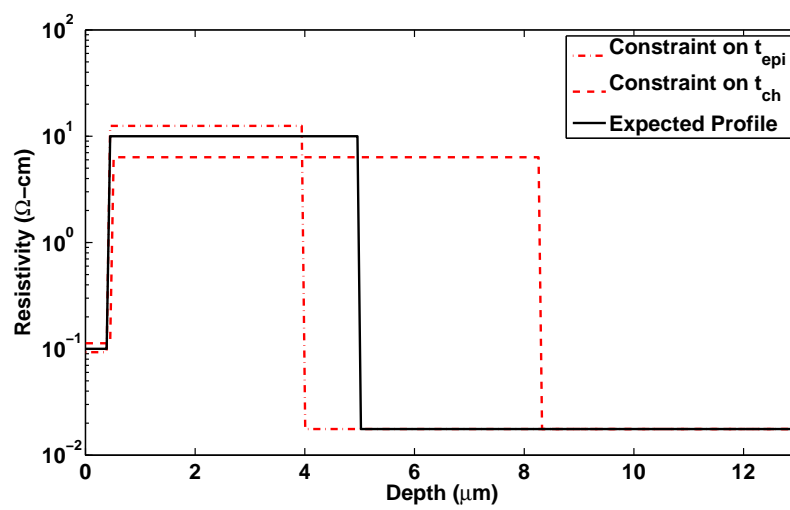


Figure 3.7: Doping profiles after calibrating with constraints on only the channel stop thickness ( $0.2\mu\text{m} \leq t_{ch} \leq 0.5\mu\text{m}$ ) and only the epi thickness ( $3.5\mu\text{m} \leq t_{epi} \leq 5\mu\text{m}$ ). For the case where  $t_{epi}$  is constrained, the final values of the channel stop and epi thickness are:  $t_{ch} = 0.41\mu\text{m}$  and  $t_{epi} = 3.57\mu\text{m}$ . For the case where  $t_{ch}$  is constrained, the final values of the channel stop and epi thickness are:  $t_{ch} = 0.5\mu\text{m}$  and  $t_{epi} = 7.8\mu\text{m}$ .

expected profile, they will still yield accurate simulation results. Multiple solutions exist because the Z-parameter values are determined by several parameters which are dependent on each other. In the case of a heavily doped substrate, the spreading in the channel as well as the resistance in the epi layer determine  $Z_{11}$ . Assuming the channel parameters are constant, there is an inverse relationship between the epi resistivity and the epi thickness. If the epi thickness goes up then the resistivity must go down to maintain a constant  $Z_{11}$  value. If the epi parameters are held constant, a linear relationship can be observed between the channel thickness and resistivity. To visualize these relationships, simulations were performed on the same contact set used for calibration where one layer is held constant and the parameters of the other layer are varied over a set range. The resulting  $Z_{11}$  values are used with measured data to calculate the sum of squared errors. Fig. 3.8 shows the plot of this error when the channel parameters are held constant and a similar plot is shown for constant epi parameters in Fig. 3.9. The valleys in these plots define the line along which solutions for the independent variables exist. Because it is difficult to see that a linear relationship between the channel stop parameters is present in this type of plot, another plot is shown in Fig. 3.10. In this plot, four different calibrations were performed and the resulting channel stop parameters are plotted against each other. It is clear from these results that a linear relationship does exist between the channel thickness and channel resistivity.

It is easy to see the relationship that exists between two parameters when the other parameters in the problem are not changing but that is not what happens in reality. For instance, when the channel stop parameters change, the line which

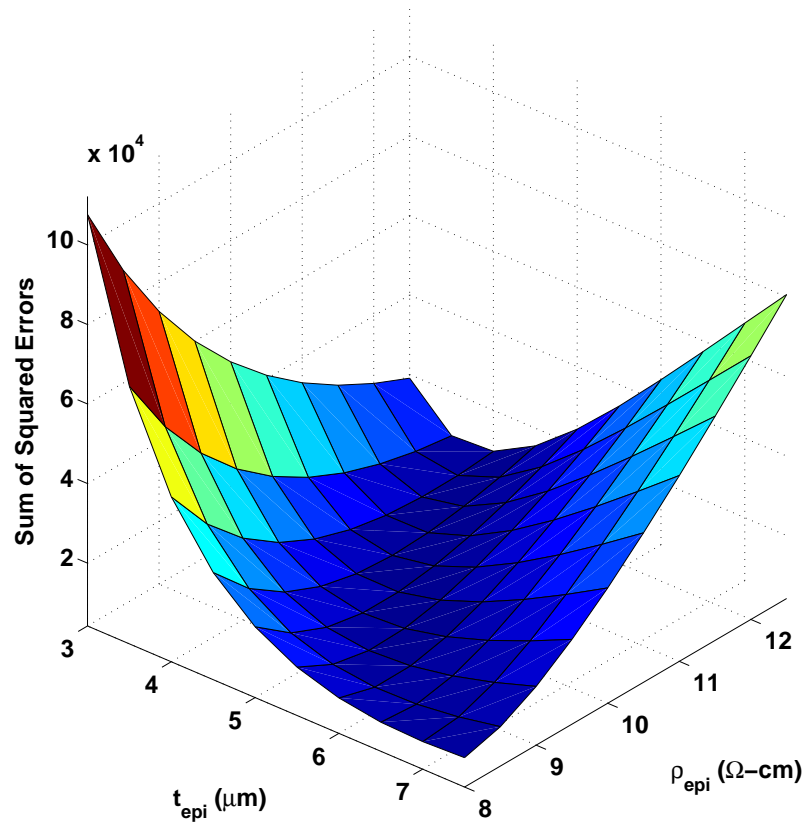


Figure 3.8: Sum of squared errors in the heavily doped substrate with constant channel stop parameters. An inverse relationship can be observed between the epi thickness and resistivity.

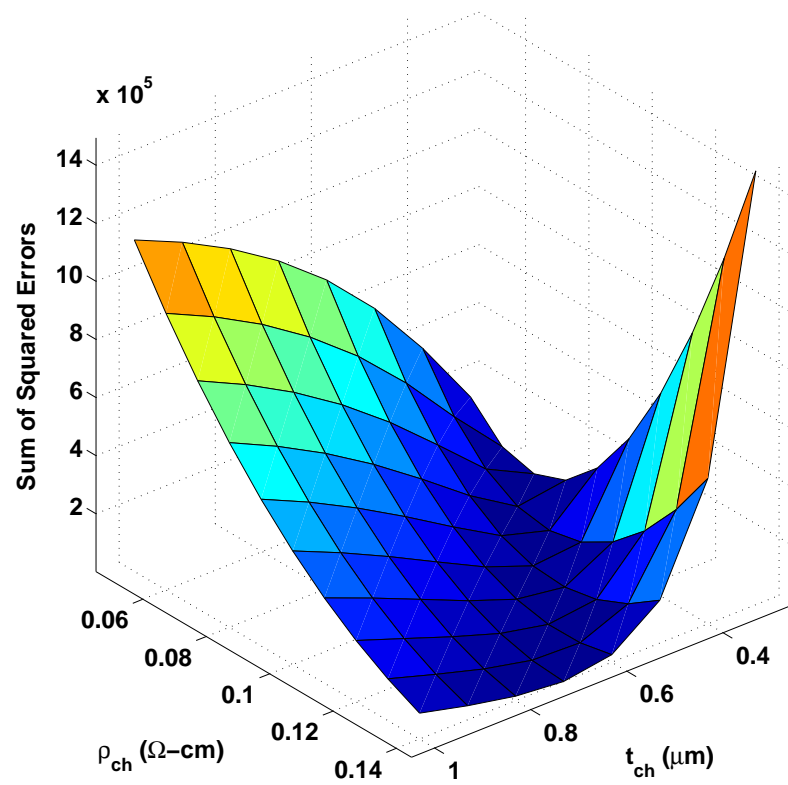


Figure 3.9: Sum of squared errors in the heavily doped substrate with constant epi layer parameters. A linear relationship can be observed between the channel thickness and resistivity.

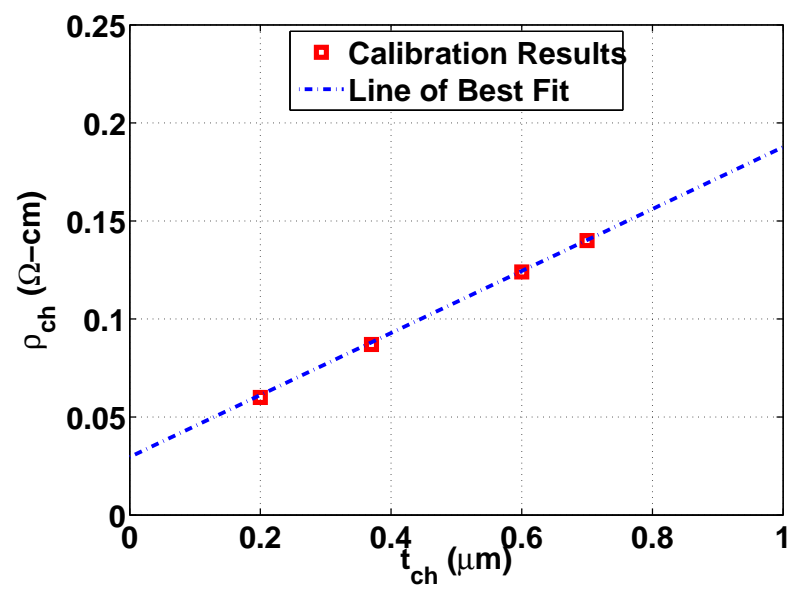


Figure 3.10: The resistivity and thickness values of the channel stop layer for four different calibrated profiles shows that a linear relationship exists for practical ranges of these parameters.

defines the relationship between the epi parameters will move. The simplest solution to this problem is simply to fix one of the parameters. Because there are multiple valid solutions, this constraint is not unreasonable. For the contacts used to calibrate the substrate,  $Z_{11}$  is less sensitive to the epi layer parameters. For this reason, it makes sense to fix one of the epi parameters. Fig. 3.11 shows the resulting profile from a calibration with the epi thickness fixed at  $4.5\mu\text{m}$ . The results from this calibration are extremely accurate because an accurate value was chosen for the epi thickness. If a reasonable range of values for the epi thickness is known, as in the constrained calibration, it is best to fix the thickness at the midpoint. This reduces the complexity and computation time of the calibration as well as improving the accuracy of the resulting profile.

### 3.3 Generating the $Z_{12}$ Dataset

With a calibrated doping profile, EPIC can be used to accurately simulate substrate parameters and can, therefore, be used to create a dataset for curve fitting. A few considerations need to be made when the contact configurations used to generate the dataset are chosen because the dataset is the foundation for the model parameter extraction. First, the limitations and the capabilities of the Z-parameter macromodel should be taken into consideration. A set of contacts should be used which include many geometric combinations that lie in the space where the model is valid and these contact cases should be simulated over a practical range of separations. For a heavily doped substrate,  $Z_{12}$  falls quickly as the separation between

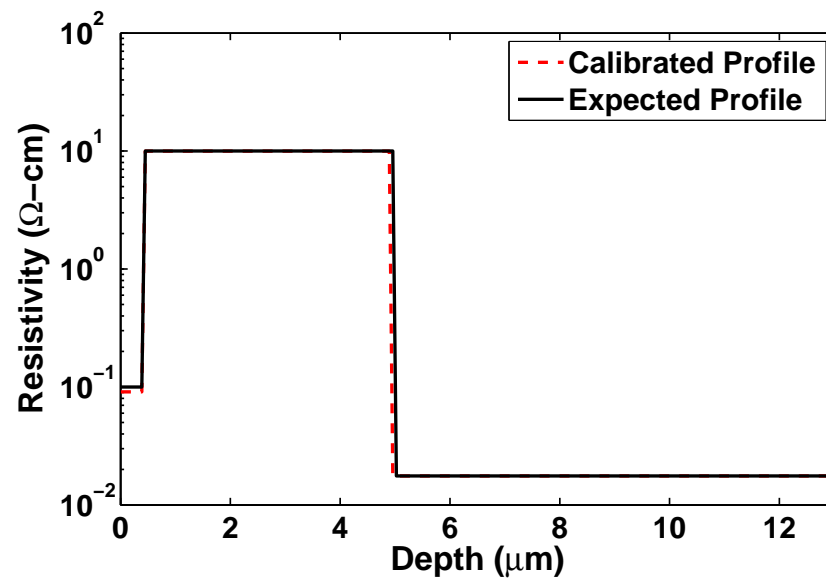


Figure 3.11: Calibration with the epi thickness fixed at  $4.5\mu\text{m}$ .

contacts increases. Thus, any separation that exceeds  $50\mu\text{m}$  or  $60\mu\text{m}$  may be superfluous. In the case of a lightly doped substrate, however, larger separations may still be relevant for curve fitting. Another consideration is the number of data points to be used. More data will result in a more accurate model, up to a certain point, but simulation time will also increase. Once a contact set has been chosen, the dataset can be generated by creating an input file for EPIC, running the simulation, and extracting the appropriate data as shown in Fig. 3.12.

### 3.4 Model Parameter Extraction

The final step in the model parameter extraction flow is to curve fit the macromodel. Once again, a LMA is employed to handle this task. Like the calibration, the parameter extraction requires an initial state which means that a set of initial values must be chosen for the process constants. Since there are no time intensive simulations during this step it is less critical that the initial values of the model parameters are close to the final values. The error function in this case is the difference between the Z-parameters calculated by the macromodel and the corresponding values from the simulated dataset. The LMA changes the values of the model parameters based on the error information and eventually the error is minimized. When the minimum error is reached, the LMA terminates and returns the final values of the model parameters. This process is illustrated in Fig. 3.13. Circuit simulation tools such as Silencer! [21] can make use of the macromodels to very quickly generate a substrate network for large SoC designs and perform

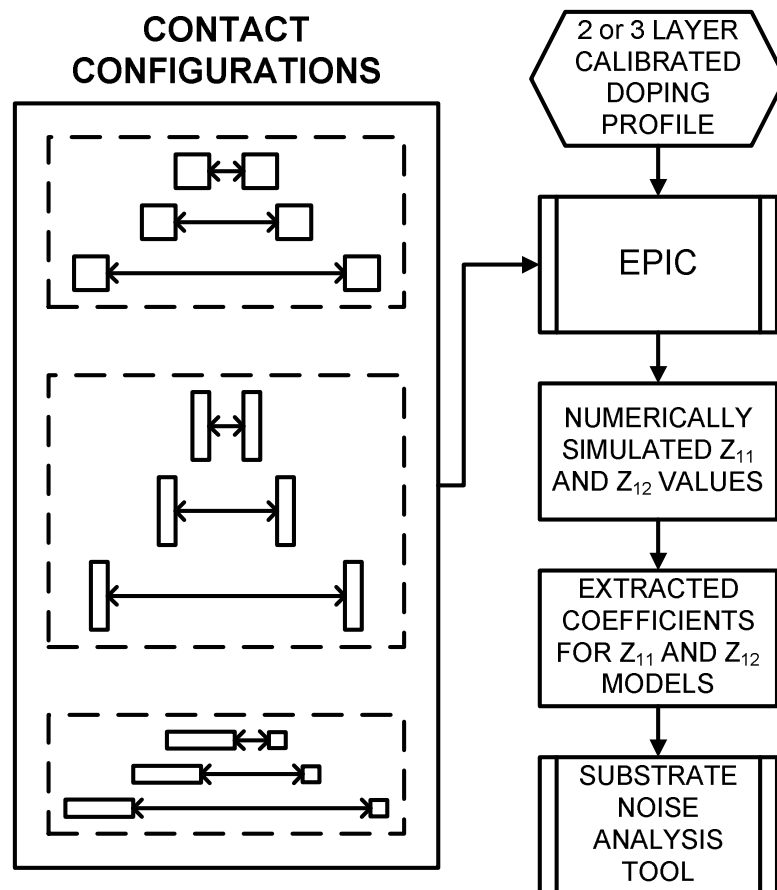


Figure 3.12: Dataset generation and model parameter extraction using a calibrated doping profile and a large variety of contact configurations.

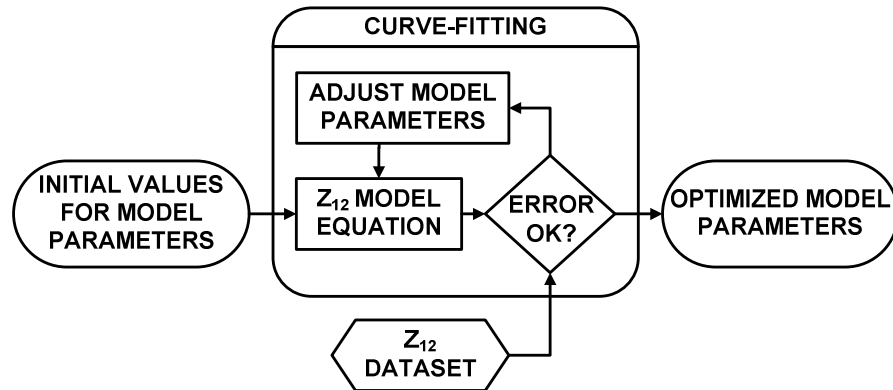


Figure 3.13: Extracting model parameters with a curve-fitting procedure.

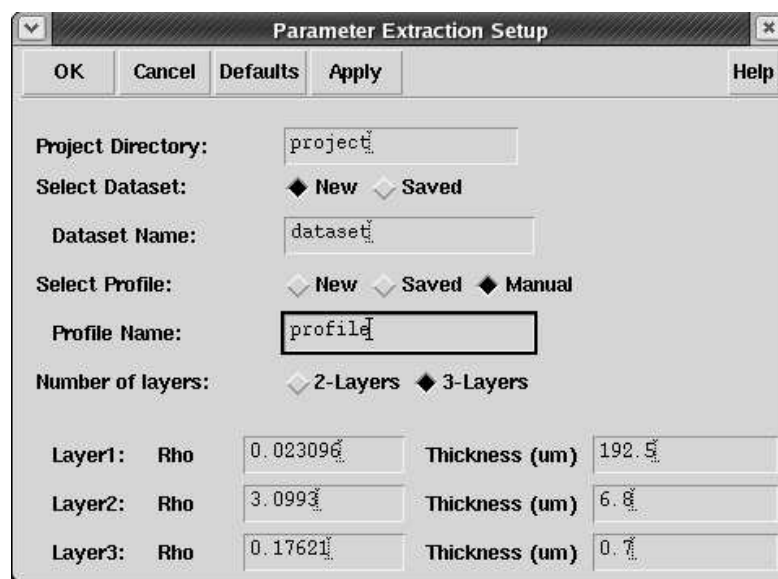
substrate noise coupling simulations.

### 3.5 Implementation in Cadence

To make the functionality of the automated model parameter extraction accessible to designers, the entire process, from calibration to parameter extraction, has been incorporated into the Cadence DFII environment. This implementation provides a seamless flow which is easily operable via the graphical user interface pictured in Fig. 3.14. Creating the calibration input file, which contains the input  $Z_{11}$  measurements, layer thickness constraints, and doping profile estimate, is the only setup required before the parameter extraction process can be started. The graphical interface allows the user to manage project data and manually configure the substrate doping profile. Also, it is possible to begin at any stage in the parameter extraction flow by using saved project data. This is advantageous if the user wishes to extract the parameters of a different model without performing

a time consuming calibration. The user can also calibrate a substrate profile for EPIC simulations without the need for dataset generation and curve fitting. This option is valuable because, if desired, Silencer! can make use of EPIC to generate a substrate network. While this is not the preferred approach, it may be necessary if a macromodel will not suffice or is not available.

The Z-parameter macromodel, which is defined in a shared object file, is customizable by the user. The interface between the model file and the parameter extraction program is simple. The parameter extraction program provides a contact configuration and a set of model parameters as an input to the model file. The equations in the model file are used with the given input to determine a  $Z_{12}$  value which is returned to the extraction program. A template for compiling a new model file makes it easy to implement different models and quickly extract their parameters. Additional details are provided in Appendix B.



The image shows a graphical user interface window titled "Parameter Extraction Setup". The window has a standard Windows-style title bar with a close button (X) on the right. Below the title bar is a menu bar with buttons for "OK", "Cancel", "Defaults", "Apply", and "Help".

The main area of the dialog contains several configuration options:

- Project Directory:** A text input field containing "project".
- Select Dataset:** Radio buttons for "New" (selected) and "Saved".
- Dataset Name:** A text input field containing "dataset".
- Select Profile:** Radio buttons for "New", "Saved", and "Manual" (selected).
- Profile Name:** A text input field containing "profile".
- Number of layers:** Radio buttons for "2-Layers" and "3-Layers" (selected).

At the bottom, there is a table for defining layer parameters:

Layer	Rho	Thickness (um)
Layer1:	0.023096	192.5
Layer2:	3.0993	6.8
Layer3:	0.17621	0.7

Figure 3.14: Graphical user interface for setting up the automated parameter extraction.

## Chapter 4 – Measurements and Validation

### 4.1 Measurements

To demonstrate that the parameter extraction flow is functional for different processes, three test chips were used. Fig. 4.1 shows the die photo of the test chip which is fabricated in a  $0.35\mu\text{m}$  CMOS process [19]. Two versions of the test chip shown in Fig. 4.2 were fabricated: one in a heavily doped  $0.25\mu\text{m}$  CMOS process and the other in a lightly doped  $0.25\mu\text{m}$  CMOS process [22]. Each test chip has a limited set of test structures which are accessible through probe pads. Z-parameter DC measurements taken on these structures are used for calibration and verification of the extracted macromodels.

The measurements taken on the  $0.35\mu\text{m}$  test chip are summarized in [19]. Measurements for the  $0.25\mu\text{m}$  test chip were taken with a HP 4156B parameter analyzer and the setup is shown in Fig. 4.3. A die perimeter ring (DPR) is used to ground the substrate and serves as a reference node for the measurements. There is a small resistance between the DPR and the backside of the substrate which affects the measurements but, for the contacts of interest, it can be ignored. This is because the contacts on the  $0.25\mu\text{m}$  test chip are relatively small and consequently have  $Z_{11}$  values which are several orders of magnitude larger than the DPR resistance. This is true for both heavily doped and lightly doped versions of the test chip.

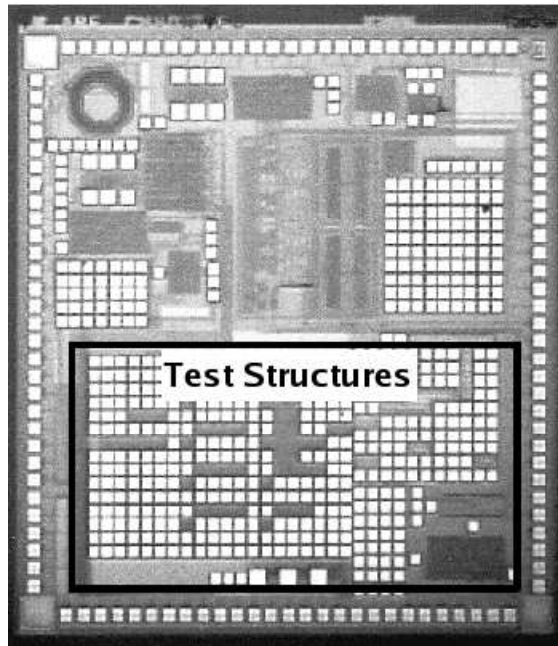


Figure 4.1: Die photo of the test chip fabricated in a  $0.35\mu\text{m}$  CMOS process.

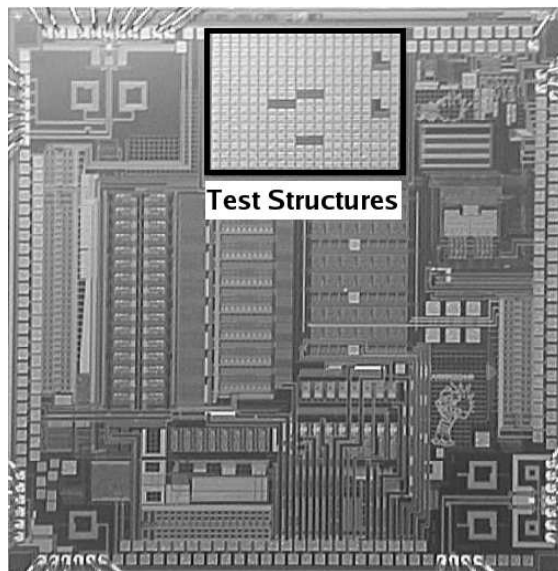


Figure 4.2: Die photo of the test chip fabricated in a  $0.25\mu\text{m}$  CMOS process.

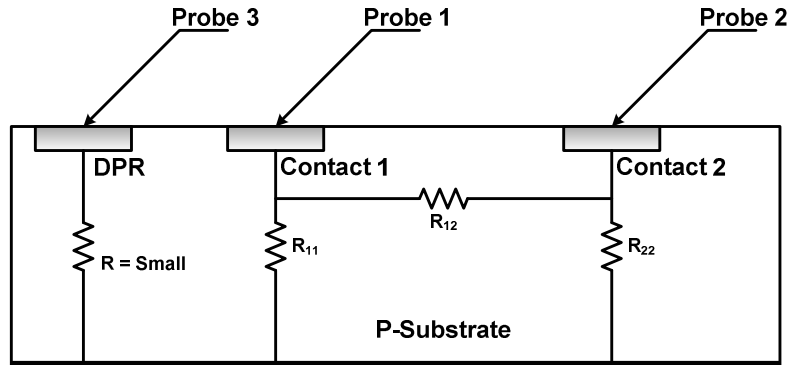


Figure 4.3: Measurement setup for the direct measurement of  $Z$ -parameters.

In the measurement setup depicted in Fig. 4.3, Probe 1 injects a current into Contact 1 and the voltage can be measured at Contact 1 to calculate  $Z_{11}$  or Contact 2 to calculate  $Z_{12}$ . Probe 3 grounds the DPR and, thus, the backside of the substrate. The current injected into Contact 1 is swept from 0-5mA and the voltage for each contact is recorded and plotted against the current. The slope of the resulting lines gives the resistance from Contact 1 to ground and the resistance between the two contacts.

## 4.2 Validating the Calibration

The calibration has been validated for all three test chips and in each case a different set of  $Z_{11}$  measurements were used. Table 4.1 contains a list of the contacts used for each process. These contact sets are not ideal based on the contact selection criteria presented in the previous chapter. However, the set of test structures for each test chip is limited and the most comprehensive set was

Table 4.1: Contact list for calibrating each substrate doping profile.

0.35 $\mu\text{m}$ Heavily Doped	0.25 $\mu\text{m}$ Heavily Doped	0.25 $\mu\text{m}$ Lightly Doped
0.7 $\mu\text{m} \times 0.7\mu\text{m}$	1 $\mu\text{m} \times 1\mu\text{m}$	0.66 $\mu\text{m} \times 0.62\mu\text{m}$
0.85 $\mu\text{m} \times 3.1\mu\text{m}$	5 $\mu\text{m} \times 5\mu\text{m}$	2 $\mu\text{m} \times 2\mu\text{m}$
1.5 $\mu\text{m} \times 1.5\mu\text{m}$	10 $\mu\text{m} \times 10\mu\text{m}$	10 $\mu\text{m} \times 10\mu\text{m}$
2.3 $\mu\text{m} \times 2.3\mu\text{m}$	20 $\mu\text{m} \times 20\mu\text{m}$	20 $\mu\text{m} \times 20\mu\text{m}$
3.1 $\mu\text{m} \times 3.1\mu\text{m}$		
6 $\mu\text{m} \times 6\mu\text{m}$		
20 $\mu\text{m} \times 40\mu\text{m}$		
60 $\mu\text{m} \times 60\mu\text{m}$		

chosen. For each process, the input doping profile estimate was chosen based on SRP data.

Using the resulting calibrated doping profiles, shown in Fig. 4.4, a set of  $Z_{12}$  simulations is performed with EPIC. These simulations are compared with measurements to show that the doping profiles are valid for  $Z_{12}$  simulations as well as  $Z_{11}$  simulations. For the 0.35 $\mu\text{m}$  test chip, measurements were taken on a pair of 0.85 $\mu\text{m} \times 1.5\mu\text{m}$  contacts and compared in Fig. 4.5 with EPIC simulations before and after calibration. Similar plots are made for each of the 0.25 $\mu\text{m}$  test chips and the same set of contacts is used in both cases. The set includes 0.66 $\mu\text{m} \times 0.62\mu\text{m}$ , 5 $\mu\text{m} \times 5\mu\text{m}$ , and 20 $\mu\text{m} \times 20\mu\text{m}$  contact pairs. Fig. 4.6 and Fig. 4.7 compare  $Z_{12}$  values from EPIC before and after calibration with measurements from heavily and lightly doped substrates, respectively. These plots show that, for all of the calibrated doping profiles, the  $Z_{12}$  values are in good agreement with measurements. And, as expected, the initial doping profile estimates yield inaccurate values for  $Z_{12}$ . After calibration, the maximum error is approximately 30% for the 0.35 $\mu\text{m}$

heavily doped substrate, 30% for the  $0.25\mu\text{m}$  heavily doped substrate and 20% for the  $0.25\mu\text{m}$  lightly doped substrate.

Errors in the calibrated profiles have a few possible origins. The substrate has been calibrated based on a small number of  $Z_{11}$  measurements and, thus, there are many possible combinations of resistivity and thickness parameters which can result from calibration. While all of these possible doping profiles may allow  $Z_{11}$  values to be simulated accurately, they may not truly represent the physical doping profile. This can affect the simulated  $Z_{12}$  values, especially when contact separations are less than about  $20\mu\text{m}$ . The  $Z_{11}$  measurements used to calibrate the substrate are fundamental to the accuracy of the output profile. Any error in the input measurements can compromise the accuracy of the calibrated substrate profile.

### 4.3 Validating the Parameter Extraction Procedure

The model parameters for each macromodel were extracted using a dataset which contains seventy different contact configurations. These contact pairs range in size from  $1.2\mu\text{m}$  to  $25\mu\text{m}$  on a side and come in many combinations of square and rectangular contacts with varying aspect ratios. Appendix A provides a complete list of contacts used for dataset generation. Each contact pair is simulated with separations over a range of  $1\mu\text{m}$  to  $50\mu\text{m}$ . After extraction, errors introduced by the model are observable by comparing the results of model calculations with EPIC simulations.

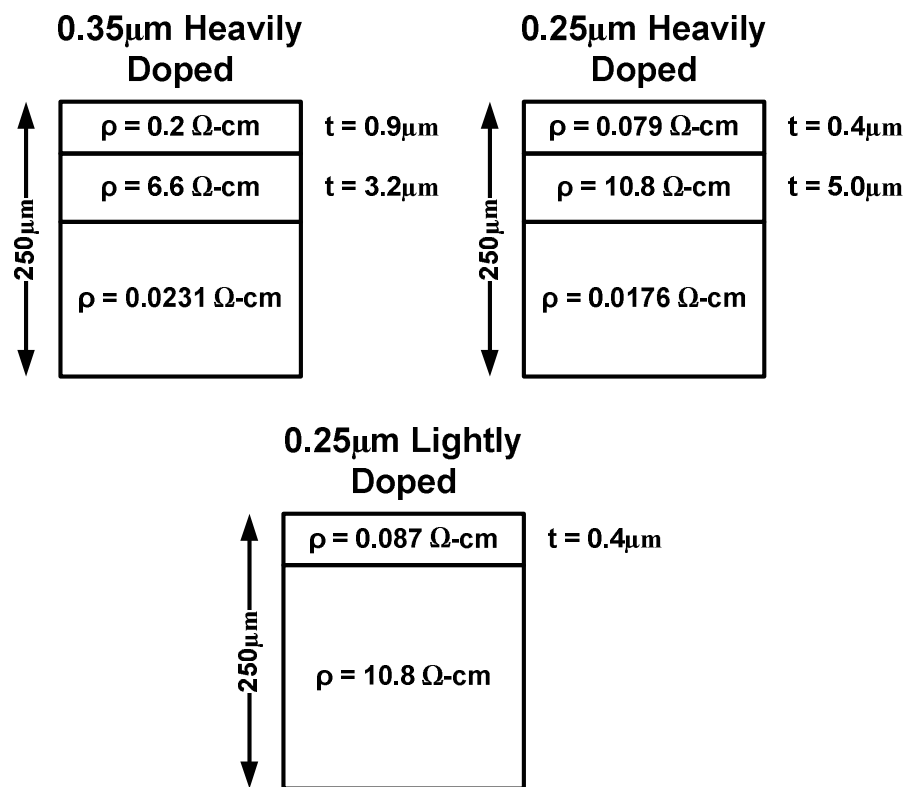


Figure 4.4: Results from the calibration of each substrate.

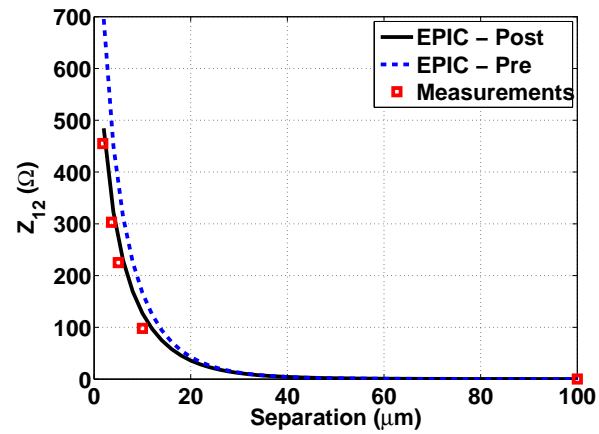


Figure 4.5: A comparison of measurements with EPIC simulations before (EPIC-Pre) and after (EPIC-Post) calibration for the  $0.35\mu\text{m}$  heavily doped substrate.

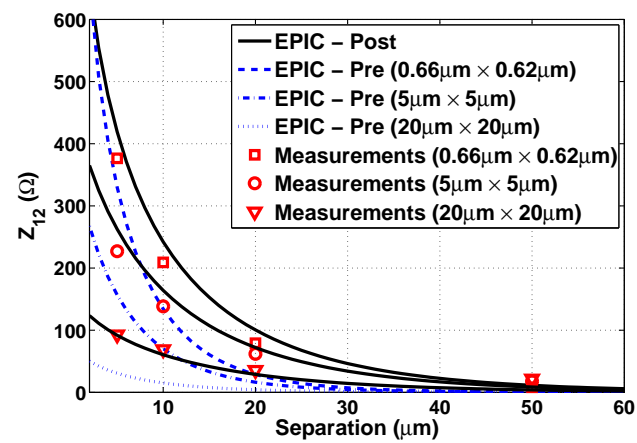


Figure 4.6: A comparison of measurements with EPIC simulations before (EPIC-Pre) and after (EPIC-Post) calibration for the  $0.25\mu\text{m}$  heavily doped substrate.

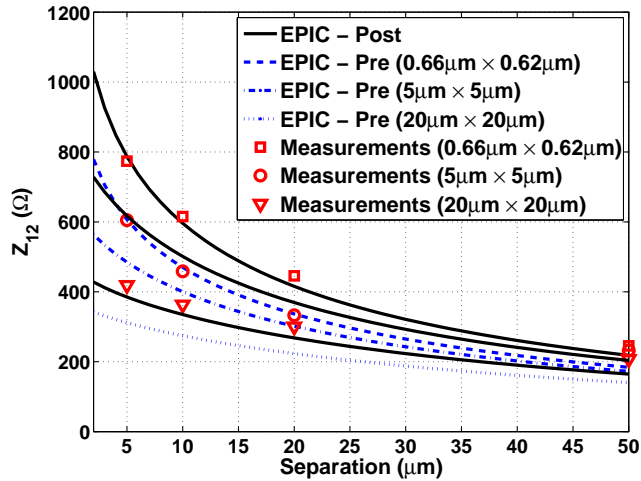


Figure 4.7: A comparison of measurements with EPIC simulations before (EPIC-Pre) and after (EPIC-Post) calibration for the lightly doped substrate.

First, the macromodels for the heavily doped substrates are tested using a dataset that was generated with the calibrated profile from the  $0.35\mu\text{m}$  process. The error plots in Fig. 4.8 show that, on average, for the macromodel defined by Equation (2.3) the error is less than half than that of the macromodel defined by Equation (2.1). Equation (2.3) is, therefore, used for all subsequent calculations in the heavily doped substrates. The maximum error is about 50% and 30% for Equations (2.1) and (2.3), respectively.

The heavily doped and lightly doped macromodels are now extracted using datasets created from the  $0.25\mu\text{m}$  doping profiles and the resulting error plots are shown in Fig. 4.9. The  $Z_{12}$  model for the heavily doped substrate has a maximum error of about 25% but on average the error falls within  $\pm 10\%$ . The errors which

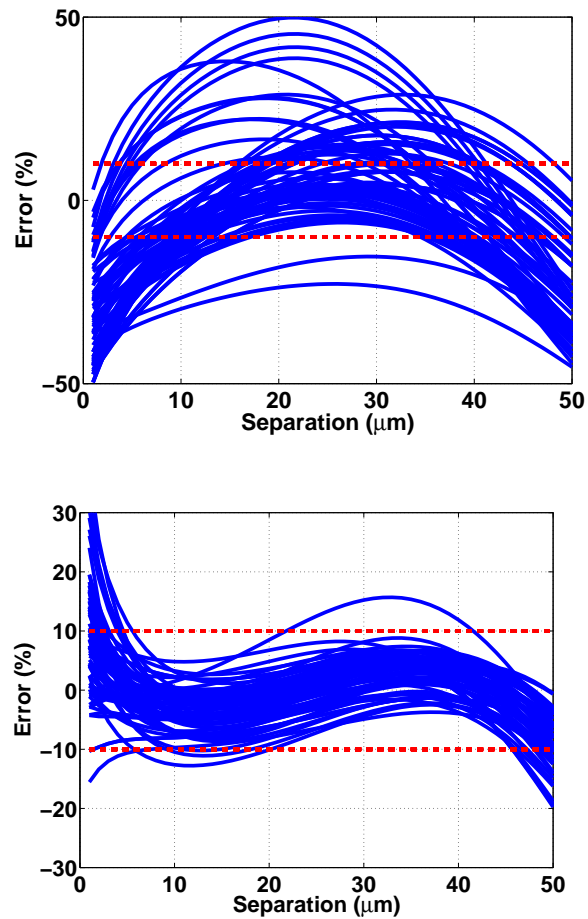


Figure 4.8: Relative error in  $Z_{12}$  versus contact separation for the heavily doped macromodel (2.1) (top) and (2.3) (bottom) after parameter extraction. Errors in these plots are reported with respect to EPIC simulations in the  $0.35\mu\text{m}$  process. Each curve represents the error for a different pair of contacts.

are greater than 10% typically come from contacts which are larger than  $20\mu\text{m}$  on a side or contacts with very large aspect ratios. The largest errors exist at separations smaller than  $5\mu\text{m}$  where the model approaches the limits of its functionality. The  $Z_{12}$  model for the lightly doped substrate has much better performance with a maximum error of 10% and an average error within  $\pm 5\%$ . In the error plot for the heavily doped substrate, the average error begins to increase close to a separation of  $45\mu\text{m}$  and appears to continue increasing after  $50\mu\text{m}$ . This is not a problem because, at these separations,  $Z_{12}$  is on the order of  $1\Omega$  which means that the coupling path will be through  $Z_{11}$ . The error in the lightly doped substrate does not appear to change dramatically at larger separations. However, a dataset which contains contacts with separations greater than  $50\mu\text{m}$  can be used if a higher level of accuracy is needed at those separations.

It is important to ensure that the dataset used for extraction is comprehensive enough to deal with any practical contact size. The maximum contact size in the dataset is  $25\mu\text{m} \times 25\mu\text{m}$  but the model must be accurate if, say, a  $100\mu\text{m} \times 100\mu\text{m}$  contact is encountered. To test this case, the parameters for the heavily doped model were extracted using the dataset given in Appendix A and the same dataset with a  $100\mu\text{m} \times 100\mu\text{m}$  contact added to it. For both sets of extracted model parameters, the average and maximum error figures and the calculated  $Z_{12}$  values for a  $100\mu\text{m} \times 100\mu\text{m}$  contact were nearly identical.

The final test is to compare the extracted macromodels with measured data. The same  $Z_{12}$  measurements that have been used to validate the calibration, which include  $0.66\mu\text{m} \times 0.62\mu\text{m}$ ,  $5\mu\text{m} \times 5\mu\text{m}$ , and  $20\mu\text{m} \times 20\mu\text{m}$  contact pairs, are used

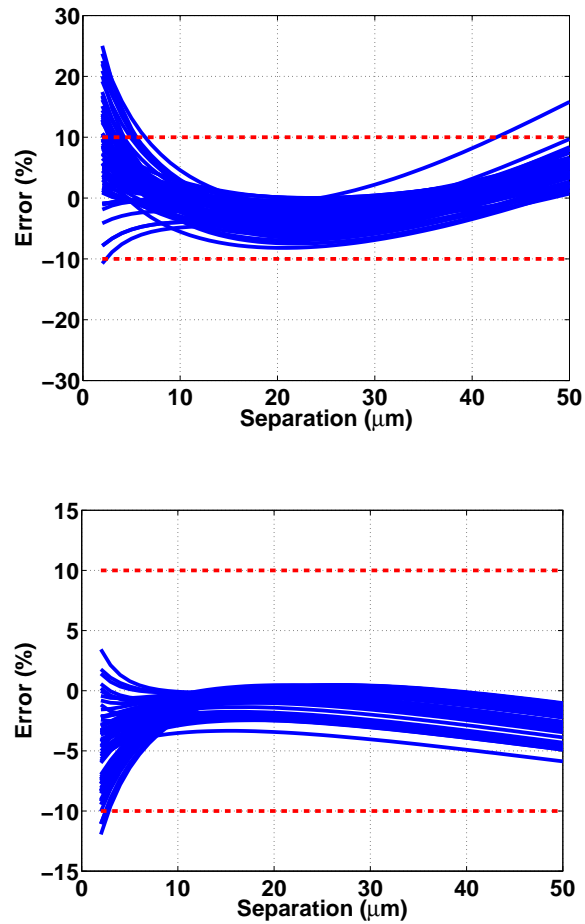


Figure 4.9: Relative error in  $Z_{12}$  versus contact separation for the heavily doped (top) and lightly doped (bottom) macromodels after parameter extraction. Errors in these plots are reported with respect to EPIC simulations in the  $0.25\mu\text{m}$  process. Each curve represents the error for a different pair of contacts.

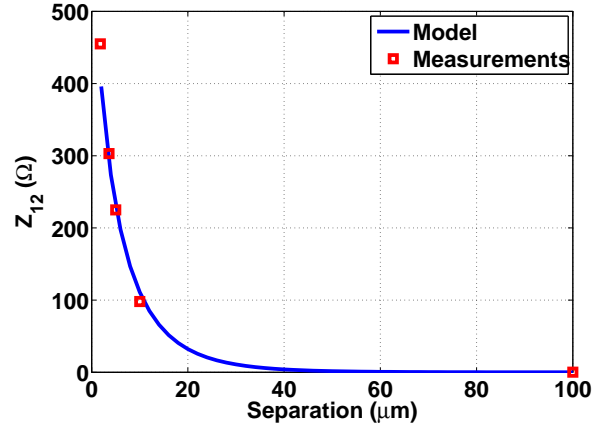


Figure 4.10: A comparison between measurements and the macromodel after extraction for the  $0.35\mu\text{m}$  heavily doped process.

again to validate the macromodel equations. Measured and calculated  $Z_{12}$  values are plotted against separation in Figs. 4.10, 4.11, and 4.12 for the  $0.35\mu\text{m}$  heavily doped process, the  $0.25\mu\text{m}$  heavily doped process, and the  $0.25\mu\text{m}$  lightly doped process, respectively. A strong correlation between the macromodel calculations and measurements is observed. The maximum error in the  $0.35\mu\text{m}$  heavily doped case is about 15% which is only coincidentally less than the error between EPIC simulations and measurements. In the case of the  $0.25\mu\text{m}$  heavily and lightly doped processes, the maximum errors are 27% and 34%, respectively. These percentage errors are very close to the errors incurred during calibration. This means that the error introduced by the macromodel is small relative to the error introduced during calibration.

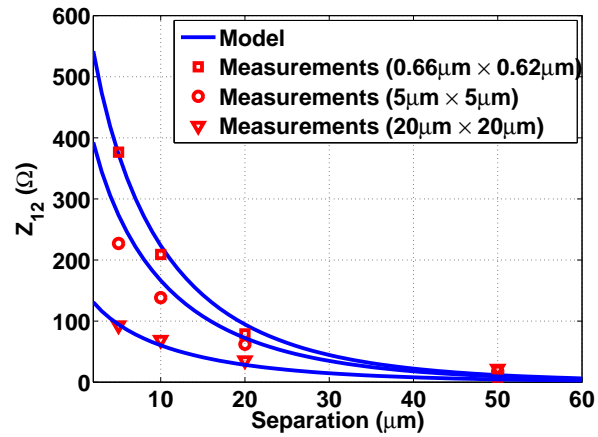


Figure 4.11: A comparison between measurements and the macromodel after extraction for the  $0.25\mu\text{m}$  heavily doped process.

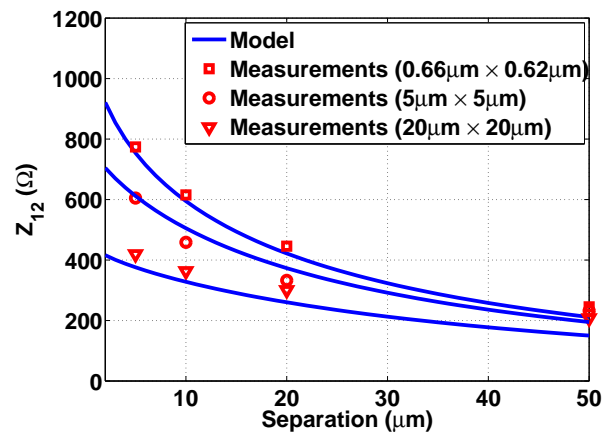


Figure 4.12: A comparison between measurements and the macromodel after extraction for the  $0.25\mu\text{m}$  lightly doped process.

## Chapter 5 – Silencer! and Assura Substrate Extraction

Silencer! [21] and Assura RCX [23] are both tools which allow designers to extract a substrate network from a circuit layout and incorporate the extracted network into SPICE simulations. Although these tools perform the same function within the Cadence platform, they implement different approaches to achieve the desired results. The following section provides a detailed comparison of the two tools.

### 5.1 Comparing Silencer! and Assura RCX

In order to compare the two tools, both are applied to a common design created in the  $0.25\mu\text{m}$  heavily doped substrate. The circuit used to compare Silencer! and Assura RCX is a stepped-buffer and an operational amplifier laid out in close proximity [24]. The distance between the edges of the two circuits is  $46\mu\text{m}$  and the distance between their centers is  $125\mu\text{m}$ . The performance of the substrate extraction as well as transient simulation results are examined when each tool is used. A clock signal applied to the stepped-buffer causes switching noise to couple through the substrate into the input of the amplifier. There is a voltage spike at the output of the amplifier due to the switching noise that couples through the power supply, ground, and package parasitics. Substrate noise will manifest itself by changing the voltage spikes at the amplifier output.

### 5.1.1 Parasitic and Substrate Extraction

One important difference between Silencer! and Assura RCX is the method of parasitic extraction. Using Assura RCX to calculate a substrate network requires a parasitic extraction with the Assura extraction tools. This means that a schematic must also be present because an LVS must be done before Assura can perform a parasitic extraction. Silencer! has no restrictions on the type of parasitic extraction that is performed. For the example used in this chapter, Silencer! uses a set of Diva extraction rules. In this example, only parasitic interconnect capacitances are extracted. However, Assura RCX requires that interconnect resistances are extracted in addition to the capacitances. The parasitic resistors can be filtered out after the extraction is done but this means that extra processing is required for the Assura extraction.

There are also differences in the substrate model used by each tool. Silencer! uses a purely resistive substrate whereas the model used by Assura RCX has resistive and capacitive elements. At frequencies below a few GHz, the capacitors in the substrate model do not play a significant role in the substrate coupling [16]. To calculate the resistor values in the substrate network, Silencer! uses EPIC, which assumes that the entire substrate is composed of three uniformly doped layers. To perform a substrate extraction with Assura RCX, SRP information is required to generate a detailed technology description file. In summary, the parasitic and substrate extraction processes and the number of extracted elements are compared in Fig. 5.1.

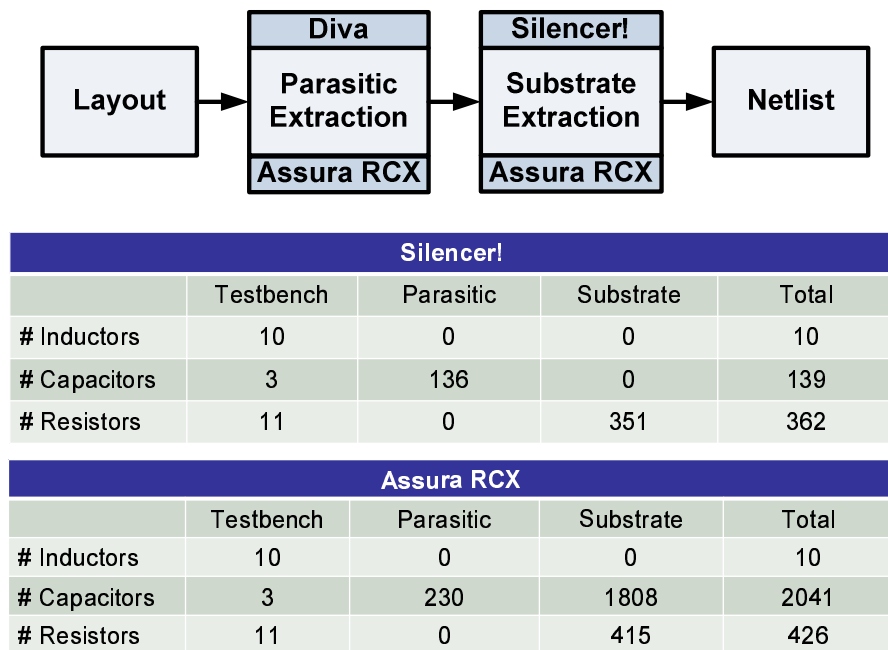


Figure 5.1: The extraction processes for Silencer! and Assura RCX and a comparison of the number of extracted elements. Assura extracts more elements for its substrate network because it uses a more complicated model.

### 5.1.2 Transient Simulations

The extracted substrate networks generated by Silencer! and Assura RCX were both used in transient simulations to observe the effects of switching noise from the stepped-buffer at the output of the operational amplifier. In both cases, the same design was simulated with the stepped-buffer running at 10MHz. The mutual inductance between bondwires in the test circuit play a significant role in the noise coupling and was modeled as in [22]. This effect is present in all of the transient simulation results presented in this section.

The waveforms from transient simulations with the substrate network generated by Assura RCX and Silencer! are compared to measurements [22] in Fig. 5.2. In this example, Silencer! comes much closer to matching the measured data than Assura RCX. The transient waveforms from Assura RCX differ from Silencer! simulations and measurements in shape and amplitude and there are several possible causes for these variations.

To explore the differences in the transient simulations, additional simulations were performed at various steps in the extraction process. Because the extraction rules are different for the two tools, it is first important to verify that the transistors and parasitics are extracted in the same manner. Simulations without a substrate network are shown in Fig. 5.3 and, as expected, there are only minor differences due to the different methods of parasitic extraction. Large discrepancies appear only when the substrate network is added, as was seen in Fig. 5.2. There is one more situation that is still worth examining. The plots in Fig. 5.4 show tran-

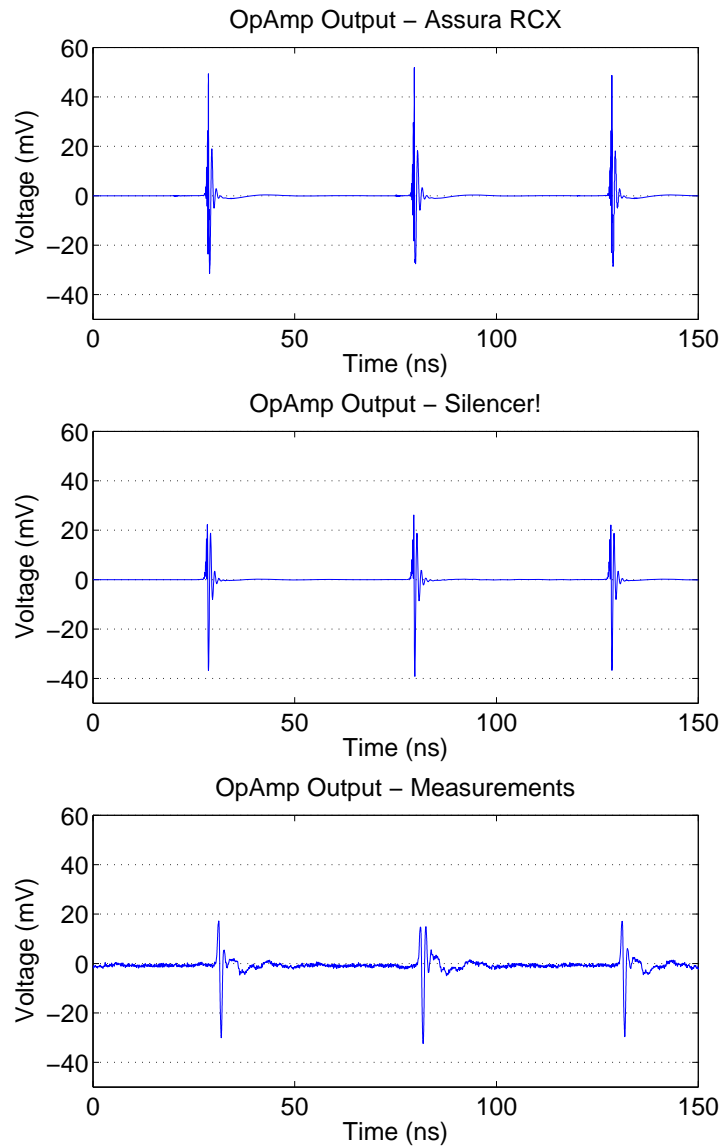


Figure 5.2: Simulated transient waveforms at the output of the op-amp with substrate networks from Assura RCX and Silencer! are compared with measurements.

sient simulations of the design when the substrate was included but the parasitic capacitors were removed. Notice that the inclusion of parasitic capacitors makes almost no difference in the substrate network from Silencer!. Assura RCX, on the other hand, varies considerably when the parasitic capacitors are removed. Not only are the substrate models different for Silencer! and Assura RCX, which can cause differences in the simulations, but the extracted parasitic capacitors from Assura RCX appear to interact with the substrate or package parasitics causing further discrepancies.

### 5.1.3 User Experience

It has been shown that Silencer! and Assura RCX are both capable of providing reasonable first order approximations of the effects of substrate noise in the example design. To compare the user experience for each tool, setup time, extraction time, and simulation time are examined. The extraction time and simulation time are both comparable for the two tools. However, it is possible to dramatically reduce the extraction time of Silencer! because a macromodel can be used to calculate the substrate network instead of numerical simulations. Also, the simulation time will always be slightly shorter when using Silencer! because the substrate model is more compact. In the example presented here, there is no noticeable difference in the simulation time because the design is small and there are a small number of extracted elements. The setup time for the two tools, however, is in no way similar. Silencer! requires only minor modifications to the extraction rules, a

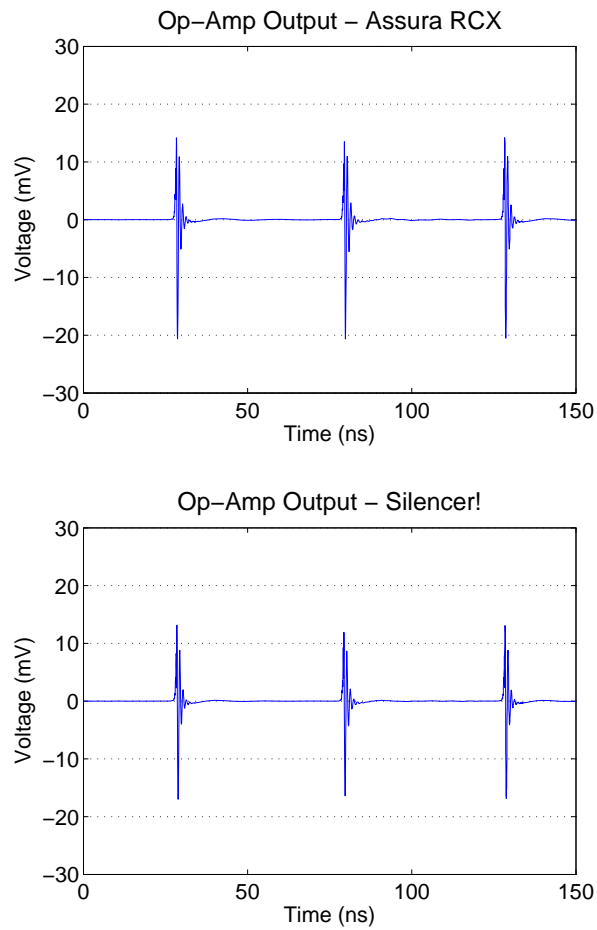


Figure 5.3: Simulated transient waveforms at the output of the op-amp without the extracted substrate network. All of the coupling in this case is a result of the mutual inductance of the bondwires.

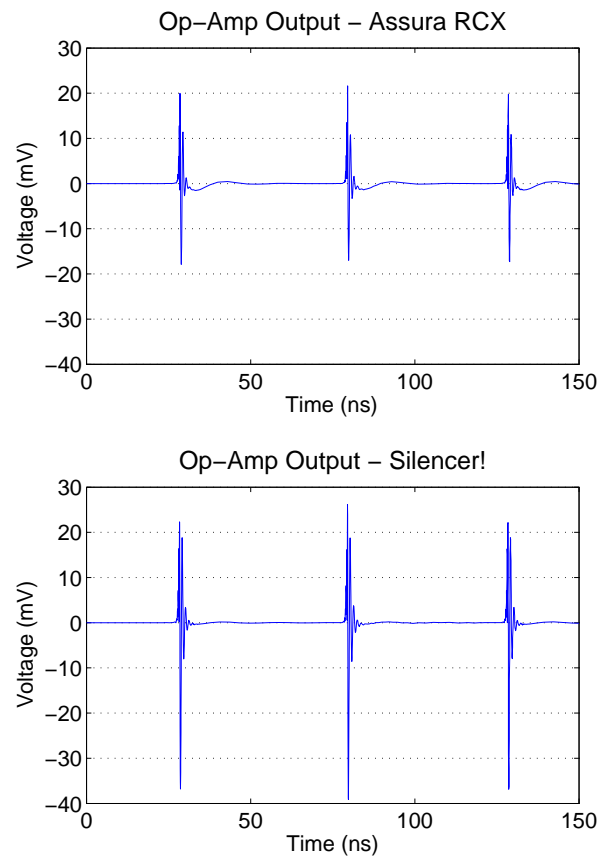


Figure 5.4: Simulated transient waveforms at the output of the op-amp with the extracted substrate network and no parasitic capacitances.

Table 5.1: A comparison of Silencer! and Assura RCX based on the design used in this chapter.

	Silencer!	Assura RCX
Setup time	~1 day	>1 week
Substrate extraction time	~3 min	~1 min
Simulation time	~10 s	~10 s
Error (this example)	~25%	~67%

job that takes no more than a few hours. Assura substrate extraction, however, requires that numerous technology files are configured in addition to the extraction rules. This is not a trivial process and requires SRP data to define the substrate. Silencer! not only has the ability to more quickly extract a substrate network, but takes less time to configure by orders of magnitude and does not require detailed substrate doping information. A summary of the parameters used to compare Silencer! and Assura RCX is given in Table 5.1.

## Chapter 6 – Conclusion

To accurately simulate substrate noise coupling, an accurate model of the substrate is needed. Many techniques exist for modeling silicon substrates but a macromodel based approach is required to efficiently model the substrate in large SoC designs. In general, macromodels cannot be easily adapted to new technologies as the model equations have many process related parameters. These parameters are not easily obtained and must be determined independently for each technology.

In this work, an automated approach for extracting the parameters of a Z-parameter macromodel, valid for both heavily and lightly doped substrates is presented. This approach makes the adaptation of macromodels to a variety of new processes a simple procedure. The parameter extraction flow has been implemented seamlessly into the Cadence DFII environment, providing designers with a tool to easily characterize a macromodel for new and upcoming technologies. Additionally, parameter extraction relies on a small amount of measured data, the majority of which is used to calibrate a substrate profile for EPIC, a numerical simulator. These features combine to form a flexible tool which can characterize an accurate substrate macromodel in an efficient and cost effective manner.

Simulation results have shown that the extracted macromodels achieve good accuracy for both heavily and lightly doped cases with maximum errors between 15% and 35%. However, improvements can be made to increase performance. In the

model parameter extraction flow there are two key sources of error. Macromodel equations are always derived based on assumptions and will, therefore, always be a source of error. In the examples presented in this work, the most significant error source is the calibration procedure. Developing solutions for deriving a substrate doping profile which are more accurate and efficient would provide the greatest increase in both performance and accuracy for the automated model parameter extraction tool. New approaches could be developed which use specific contact arrangements to extract the channel-stop or epi layer parameters independently. This could lead to faster extraction times, more accurate doping profile estimates, and a smaller set of required input data. Developing new macromodels which are more accurate and robust will also lead to more accurate analysis. Future work could also include the extension of the automated model parameter extraction approach to other numerical simulators and design environments as well as validation with deep-submicron CMOS technologies and high frequency substrate models.

## Bibliography

- [1] D. K. Su, M. J. Loinaz, S. Masui, and B. A. Wooley, "Experimental results and modeling techniques for substrate noise in mixed-signal integrated circuits," *IEEE J. Solid-State Circuits*, vol. 28, pp. 420–430, 1993.
- [2] N. K. Verghese, T. J. Schmerbeck, and D. J. Allstot, *Simulation Techniques and Solutions for Mixed-Signal Coupling in Integrated Circuits*. Kluwer Academic Publishers, 1995.
- [3] I. L. Wemple and A. T. Yang, "Integrated circuit substrate coupling models based on Voronoi tessellation," *IEEE Trans. Computer-Aided Design*, vol. 14, pp. 1459–1469, Dec. 1995.
- [4] R. Gharpurey and R. G. Meyer, "Modeling and analysis of substrate coupling in integrated circuits," *IEEE J. Solid-State Circuits*, vol. 31, pp. 344–353, Mar. 1996.
- [5] J. P. Costa, M. Chou, and L. M. Silveira, "Efficient techniques for accurate modeling and simulation of substrate coupling in mixed-signal IC's," *IEEE Trans. Computer-Aided Design*, vol. 18, pp. 597–607, May 1999.
- [6] B. R. Stanisic, N. K. Verghese, R. A. Rutenbar, R. L. Carley, and D. J. Allstot, "Addressing substrate coupling in mixed-mode IC's and power distribution synthesis," *IEEE J. Solid-State Circuits*, vol. 29, pp. 226–237, Mar. 1994.
- [7] T. A. Johnson, R. W. Knepper, V. Marcello, and W. Wang, "Chip substrate resistance modeling technique for integrated circuit design," *IEEE Trans. Computer-Aided Design*, vol. CAD-3, pp. 126–134, 1984.
- [8] E. Schrik and N. van der Meijs, "Combined BEM/FEM substrate resistance modeling," in *Proc. DAC*, June 2002, pp. 771–776.
- [9] D. Ozis, T. Fiez, and K. Mayaram, "A comprehensive geometry-dependent macromodel for substrate noise coupling in heavily doped CMOS processes," in *Proc. IEEE CICC*, May 2002, pp. 497–500.

- [10] S. K. Arunachalam, "An efficient and accurate method of estimating substrate noise coupling in heavily doped substrates," Master's Thesis, Oregon State University, Aug. 2005.
- [11] K. Srinivasan, "Computationally efficient substrate noise coupling estimation in lightly doped substrates," Master's Thesis, Oregon State University, Sept. 2006.
- [12] A. Samavedam, A. Sadate, K. Mayaram, and T. Fiez, "A scalable substrate noise coupling model for design of mixed-signal IC's," *IEEE J. Solid-State Circuits*, vol. 35, pp. 895–904, June 2000.
- [13] A. van Genderen, N. van der Meijs, and T. Smedes, "Fast computation of substrate resistances in large circuits," in *Proc. European Design and Test Conference*, Mar. 1996, pp. 560–565.
- [14] S. Kristiansson, F. Ingvarson, S. P. Kagganti, N. Simić, M. Zgrda, and K. O. Jeppson, "A surface potential model for predicting substrate noise coupling in integrated circuits," *IEEE J. Solid-State Circuits*, vol. 40, pp. 1797–1803, Sept. 2005.
- [15] N. K. Verghese, D. J. Allstot, and M. A. Wolfe, "Fast parasitic extraction for substrate coupling in mixed-signal IC's," in *Proc. IEEE CICC*, May 1995, pp. 121–124.
- [16] N. K. Verghese and D. J. Allstot, "Computer-aided design considerations for mixed-signal coupling in RF integrated circuits," *IEEE J. Solid-State Circuits*, vol. 33, pp. 314–323, Mar. 1998.
- [17] H. Lan, T. W. Chen, C. O. Chui, and R. W. Dutton, "Compact modeling and experimental verification of substrate resistance in lightly doped substrates," in *Proc. SASIMI*, Oct. 2004, pp. 189–195.
- [18] C. Xu, *EPIC: A Program for Extraction of the Resistance and Capacitance of Substrate With the Green's Function Method*, ECE Dept., Oregon State Univ., 2002.
- [19] A. Sharma, P. Birrer, S. K. Arunachalam, C. Xu, T. S. Fiez, and K. Mayaram, "Accurate prediction of substrate parasitics in heavily doped CMOS processes using a calibrated boundary element solver," *IEEE Trans. VLSI*, vol. 13, pp. 843–851, July 2005.

- [20] D. Marquardt, “An algorithm for least-squares estimation of nonlinear parameters,” *SIAM J. App. Math.*, vol. 11, pp. 431–441, June 1963.
- [21] P. Birrer, T. S. Fiez, and K. Mayaram, “Silencer!: A tool for substrate noise coupling analysis,” in *Proc. IEEE International SOC Conference*, Sept. 2004, pp. 105–108.
- [22] J. S. Ayers, “A comparison of substrate noise coupling in heavily doped and lightly doped substrates for mixed-signal circuits,” Master’s Thesis, Oregon State University, June 2004.
- [23] *Assura Physical Verification User Guide*, Cadence Design Systems, Inc., 2006.
- [24] B. E. Owens, “Simulation, measurement, and suppression of digital noise in mixed-signal integrated circuits,” Master’s Thesis, Oregon State University, Sept. 2003.

APPENDICES

## Appendix A – Contact Pairs Used for Dataset Generation

Table A.1 contains a list of contact pairs used to generate the simulated dataset for model parameter extraction. Each of these contact pairs is varied in separation from  $1\mu\text{m}$  to  $50\mu\text{m}$  in increments of  $1\mu\text{m}$  resulting in 3430 data points in total.

Table A.1: Contact pairs used to simulate  $Z_{12}$  values for the dataset from which model parameters are extracted.

Contact A ( $\mu\text{m} \times \mu\text{m}$ )	Contact B ( $\mu\text{m} \times \mu\text{m}$ )	Contact A ( $\mu\text{m} \times \mu\text{m}$ )	Contact B ( $\mu\text{m} \times \mu\text{m}$ )
1.2 $\times$ 1.2	1.2 $\times$ 1.2	2.0 $\times$ 2.0	2.0 $\times$ 2.0
3.0 $\times$ 3.0	3.0 $\times$ 3.0	4.0 $\times$ 4.0	4.0 $\times$ 4.0
5.0 $\times$ 5.0	5.0 $\times$ 5.0	6.0 $\times$ 6.0	6.0 $\times$ 6.0
8.0 $\times$ 8.0	8.0 $\times$ 8.0	10.0 $\times$ 10.0	10.0 $\times$ 10.0
12.0 $\times$ 12.0	12.0 $\times$ 12.0	14.0 $\times$ 14.0	14.0 $\times$ 14.0
16.0 $\times$ 16.0	16.0 $\times$ 16.0	18.0 $\times$ 18.0	18.0 $\times$ 18.0
20.0 $\times$ 20.0	20.0 $\times$ 20.0	20.0 $\times$ 20.0	5.0 $\times$ 5.0
20.0 $\times$ 5.0	5.0 $\times$ 5.0	20.0 $\times$ 5.0	20.0 $\times$ 5.0
20.0 $\times$ 5.0	5.0 $\times$ 20.0	2.0 $\times$ 2.0	5.0 $\times$ 5.0
2.0 $\times$ 5.0	5.0 $\times$ 2.0	2.0 $\times$ 2.0	3.0 $\times$ 3.0
4.0 $\times$ 3.6	2.8 $\times$ 3.2	2.5 $\times$ 3.0	4.0 $\times$ 2.0
6.0 $\times$ 8.0	9.0 $\times$ 5.0	10.0 $\times$ 16.0	3.0 $\times$ 3.0
25.0 $\times$ 7.0	16.0 $\times$ 20.0	18.0 $\times$ 14.0	3.6 $\times$ 2.5
3.0 $\times$ 1.0	2.0 $\times$ 2.4	4.0 $\times$ 3.6	2.8 $\times$ 1.2
4.0 $\times$ 2.0	4.0 $\times$ 2.0	1.0 $\times$ 2.0	2.0 $\times$ 2.0
2.0 $\times$ 5.0	3.0 $\times$ 3.0	3.0 $\times$ 5.0	2.0 $\times$ 4.5
10.0 $\times$ 10.0	5.0 $\times$ 4.0	15.0 $\times$ 12.0	8.0 $\times$ 20.0
20.0 $\times$ 2.0	5.0 $\times$ 8.0	20.0 $\times$ 10.0	20.0 $\times$ 10.0
6.0 $\times$ 3.0	6.0 $\times$ 3.0	10.0 $\times$ 5.0	10.0 $\times$ 5.0
2.4 $\times$ 1.2	2.4 $\times$ 1.2	16.0 $\times$ 18.0	25.0 $\times$ 18.0
5.0 $\times$ 19.0	4.0 $\times$ 16.0	6.0 $\times$ 9.0	8.0 $\times$ 12.0
20.0 $\times$ 2.0	20.0 $\times$ 2.0	20.0 $\times$ 4.0	20.0 $\times$ 4.0
20.0 $\times$ 3.0	20.0 $\times$ 3.0	18.0 $\times$ 10.0	2.0 $\times$ 10.0
15.0 $\times$ 10.0	5.0 $\times$ 10.0	10.0 $\times$ 18.0	10.0 $\times$ 2.0
10.0 $\times$ 15.0	10.0 $\times$ 5.0	18.0 $\times$ 15.0	2.0 $\times$ 5.0
18.0 $\times$ 5.0	2.0 $\times$ 15.0	18.0 $\times$ 18.0	2.0 $\times$ 2.0
18.0 $\times$ 2.0	2.0 $\times$ 18.0	15.0 $\times$ 18.0	5.0 $\times$ 2.0
15.0 $\times$ 2.0	5.0 $\times$ 18.0	15.0 $\times$ 15.0	5.0 $\times$ 5.0
15.0 $\times$ 5.0	5.0 $\times$ 15.0	20.0 $\times$ 2.0	2.0 $\times$ 2.0
2.0 $\times$ 20.0	2.0 $\times$ 2.0	10.0 $\times$ 3.0	3.0 $\times$ 16.0
25.0 $\times$ 20.0	16.0 $\times$ 7.0	18.0 $\times$ 2.5	3.6 $\times$ 14.0
3.0 $\times$ 2.4	2.0 $\times$ 1.0	4.0 $\times$ 1.2	2.8 $\times$ 3.6
4.0 $\times$ 2.0	4.0 $\times$ 2.0	2.0 $\times$ 2.0	1.0 $\times$ 2.0
3.0 $\times$ 5.0	2.0 $\times$ 3.0	2.0 $\times$ 5.0	3.0 $\times$ 4.5
5.0 $\times$ 10.0	10.0 $\times$ 4.0	25.0 $\times$ 25.0	25.0 $\times$ 25.0

## Appendix B – Implementing a New Macromodel

The LMA which is used to optimize the macromodel parameters has been implemented in C. The function which calculates  $Z_{12}$  based on the model equations is contained in a shared object which makes the macromodel definition independent from the model parameter extraction program. Shared objects are dynamically linked to by the calling program which allows the macromodel to be changed without having to recompile the main program. The interface between the main program and the shared object, as shown in Fig. B.1, is simple. Data describing the configuration of a particular contact pair, which defines the shape, size, and separation of the contacts, is passed to the function in the shared object. At this point,  $Z_{12}$  for the contact pair is calculated and can be used in the main program.

The function defining the model equations is defined as a standard C function. The example below implements the  $Z_{12}$  model for heavily doped substrates.

$$Z_{12} = \alpha e^{\beta x^{0.75}} \quad (\text{B.1})$$

In the following code example, the parameters  $lx1$ ,  $ly1$ ,  $lx2$ , and  $ly2$  define the side length of contact 1 and contact 2 in the x and y directions, respectively.  $x\_sep$  is the separation between the two contacts and  $c$  is an array containing the process related constants.  $ans$  holds the calculated value of  $Z_{12}$  which is used by the calling

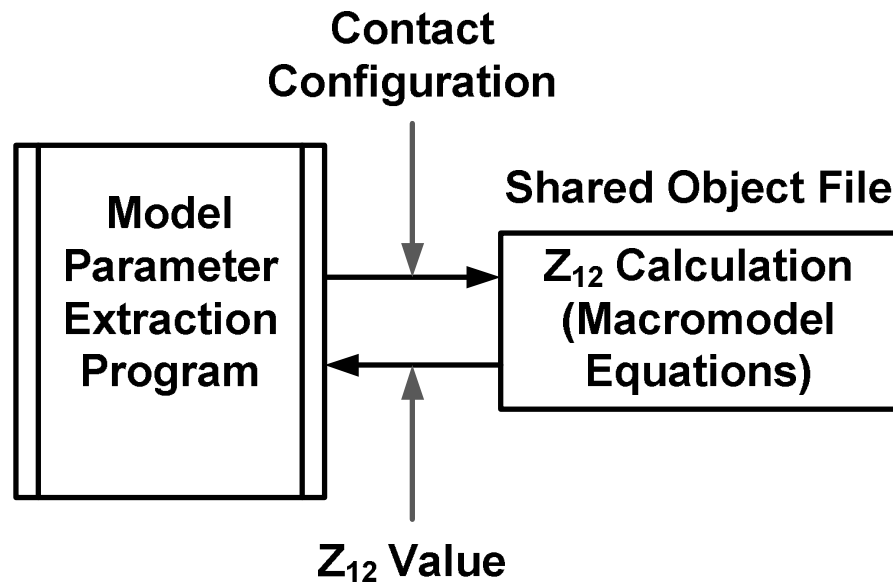


Figure B.1: The interface between the parameter extraction code and the shared object.

program.

```

/***** model_calc.c *****/
#include "math.h"
int model_calc(float *contact_geom, float *c, float *ans){
    float a, b, lx1, lx2, ly1, ly2, x_sep;
    lx1 = contact_geom[0];
    ly1 = contact_geom[1];
    lx2 = contact_geom[2];
    ly2 = contact_geom[3];
    x_sep = contact_geom[4];
    a = (1/(c[0]*pow((lx1 + lx2),c[1]) + c[2]*pow((ly1 + ly2),c[3])

```

```
    + c[4]*((lx1 + lx2)*(ly1 + ly2)) + c[5]));  
b = (1/(c[6]*(2*(lx1 + ly1 + lx2 + ly2)) + c[7]));  
*ans = a*exp(-b*pow(x_sep,0.75));  
return 1;  
} //end model_calc
```

The following shell script is used to compile the shared object file.

```
#!/bin/csh  
  
if ( -e model_calc.o ) then  
    rm model_calc.o  
endif  
  
gcc -c -fpic model_calc.c  
  
if ( -e model_calc.so ) then  
    rm model_calc.so  
endif  
  
gcc -shared -lc -lm -o model_calc.so model_calc.o
```

## Appendix C – Model Parameter Extraction With Silencer!

This appendix describes the additions made to Silencer! in order to implement the automated model parameter extraction flow. None of the existing Silencer! code was changed except that a menu item was added to allow access to the calibration, dataset generation, and parameter extraction functions. Wrapper scripts for these functions are called via a graphical user interface described in the following Skill code.

```
;; Title: Substrate Characterization Tool
;; DESCRIPTION: Contains a GUI with functions to:
;;-Calibrate a 2- or 3-layer profile to be used with EPIC
;;-Generate a dataset of Z12 values
;;-Fit a macromodel to the dataset
```

```
(defun sncModelfit ()
  printf("Extracting Model Parameters\n")
  cid = ipcSkillProcess( sprintf( nil,
    "Silencer/sub_char/bin/modelfit %s/%s %s/params.txt",
    sModelfitSetup->project_name->value,
```

```
sModelfitSetup->data_saved->value,  
sModelfitSetup->pject_name->value))  
ipcWait(cid)  
)
```

```
(defun sncDataset ()  
printf("Generating Dataset\n")  
cid = ipcSkillProcess( sprintf( nil,  
"Silencer/sub_char/bin/dataset %s %s %s",  
sModelfitSetup->pject_name->value,  
sModelfitSetup->profile_name->value,  
sModelfitSetup->data_saved->value))  
ipcWait(cid 600 100000)  
)
```

```
(defun sncCalibrate ()  
printf("Calibrating the Substrate Profile\n")  
cid = ipcSkillProcess( sprintf( nil,  
"Silencer/sub_char/bin/calibrate %s %s",  
sModelfitSetup->pject_name->value,  
sModelfitSetup->profile_name->value))  
ipcWait(cid 3600 1000000)  
)
```

```

(defun sncWriteProfile ()
  out = outfile(sprintf(nil
    "Silencer/sub_char/projects/%s/%s"
    sModelfitSetup->project_name->value
    sModelfitSetup->profile_name->value) "w")
  fprintf(out "%1.4e\t%.2f\n"
    sModelfitSetup->lay1r->value
    sModelfitSetup->lay1t->value)
  fprintf(out "%1.4e\t%.2f\n"
    sModelfitSetup->lay2r->value
    sModelfitSetup->lay2t->value)
  (if sModelfitSetup->num_layers->value == "3-Layers"
    then
    fprintf(out "%1.4e\t%.2f"
      sModelfitSetup->lay3r->value
      sModelfitSetup->lay3t->value)
    )
  close(out)
)

(defun sncFileCheck (dir, file1)
  let( (stat str)

```

```

cid = (ipcSkillProcess (sprintf nil
"Silencer/sub_char/bin/fileCheck
Silencer/sub_char/projects/%s
Silencer/sub_char/projects/%s/%s" dir dir file1))
stat = 0
sprintf(str "%s\n" ipcReadProcess(cid,1))
(if strcmp(str, "ERROR") == 1
stat = 1
)
stat
)
)

(defun sncExec ()
(if sModelfitSetup->data_select->value == "Saved"
then
(if sncFileCheck(sModelfitSetup->project_name->value
sModelfitSetup->data_saved->value) == 1
then
sncInfoDialog("Error reading one or more files")
else
sncModelfit()
);endif

```

```
else
  (if sModelfitSetup->profile_select->value == "Saved"
    (if sncFileCheck(sModelfitSetup->pject_name->value
      sModelfitSetup->profile_name->value) == 1
      then
        sncInfoDialog("Error reading one or more files")
      else
        sncDataset()
        sncModelfit()
      );endif
    );endif

  (if sModelfitSetup->profile_select->value == "New"
    then
      sncFileCheck(sModelfitSetup->pject_name->value "" )
      sncCalibrate()
      sncDataset()
      sncModelfit()
    );endif

  (if sModelfitSetup->profile_select->value == "Manual"
    then
```

```

sncFileCheck(sModelfitSetup->pject_name->value "" )
sncWriteProfile()
sncDataset()
sncModelfit()
);endif
);endif

err = infile("./Silencer/sub_char/bin/
param_extract/model_error.txt")
fscanf( err "%f" error)
sncInfoDialog( sprintf(nil "Operation complete!\n
Maximum error in the model is : %.1f%%" error))

cid = ipcSkillProcess( sprintf( nil,
"Silencer/sub_char/bin/clean"))
ipcWait(cid)
)

(defun sncRunCalib ()
sncFileCheck(sCalibSetup->pject_name->value "")
cid = ipcSkillProcess( sprintf( nil,
"Silencer/sub_char/bin/calibrate %s %s",
sCalibSetup->pject_name->value,

```

```
sCalibSetup->profile_name->value))
ipcWait(cid 3600 1000000)
sncInfoDialog("Operation complete")
)

(defun setEdit ()
  (if sModelfitSetup->data_select->value == "New"
    then
      sModelfitSetup->profile_select->enabled = 't
    else
      sModelfitSetup->profile_select->enabled = 'nil
  )
  (if sModelfitSetup->profile_select->enabled == 'nil
    then
      sModelfitSetup->profile_name->editable = 'nil
      sModelfitSetup->num_layers->enabled = 'nil
    else
      sModelfitSetup->profile_name->editable = 't
  )
  (if sModelfitSetup->profile_select->value == "Manual" &&
    sModelfitSetup->profile_select->enabled == 't
  then
```

```
sModelfitSetup->num_layers->enabled = 't
sModelfitSetup->lay1r->enabled = 't
sModelfitSetup->lay1t->enabled = 't
sModelfitSetup->lay2r->enabled = 't
sModelfitSetup->lay2t->enabled = 't
(if sModelfitSetup->num_layers->value == "2-Layers"
then
sModelfitSetup->lay3r->enabled = 'nil
sModelfitSetup->lay3t->enabled = 'nil
else
sModelfitSetup->lay3r->enabled = 't
sModelfitSetup->lay3t->enabled = 't
)

else
sModelfitSetup->num_layers->enabled = 'nil
sModelfitSetup->lay1r->enabled = 'nil
sModelfitSetup->lay1t->enabled = 'nil
sModelfitSetup->lay2r->enabled = 'nil
sModelfitSetup->lay2t->enabled = 'nil
sModelfitSetup->lay3r->enabled = 'nil
sModelfitSetup->lay3t->enabled = 'nil
)
```

```
)
```

```
(defun sncModelfitGUI ()
```

```
  project_name= (hiCreateStringField
```

```
    ?name'project_name
```

```
    ?value "substrate1"
```

```
    ?prompt"Project Directory:"
```

```
)
```

```
  data_select = (hiCreateRadioField
```

```
    ?name'data_select
```

```
    ?value "Saved"
```

```
    ?prompt "Select Dataset: "
```

```
    ?choices (list "New" "Saved")
```

```
    ?callback (list "(setEdit)")
```

```
)
```

```
  data_saved= (hiCreateStringField
```

```
    ?name'data_saved
```

```
    ?prompt "Dataset Name: "
```

```
?value "dataset"
```

```
)
```

```
profile_select= (hiCreateRadioField
```

```
?name'profile_select
```

```
?value "Saved"
```

```
?prompt "Select Profile:"
```

```
?choices (list "New" "Saved" "Manual")
```

```
?enabled 'nil
```

```
?callback (list "(setEdit)")
```

```
)
```

```
profile_name= (hiCreateStringField
```

```
?name'profile_name
```

```
?prompt "Profile Name: "
```

```
?value "profile"
```

```
?editable 'nil
```

```
)
```

```
num_layers= (hiCreateRadioField
```

```
?name'num_layers
```

```
?value"3-Layers"
```

```
?prompt"Number of layers:"
```

```
?choices (list "2-Layers" "3-Layers")
?enabled 'nil
?callback (list "(setEdit)")
)
```

```
s_floatField1 = hiCreateFloatField(
?name 'lay1r
?prompt "Layer1:      Rho "
?enabled 'nil
?value.023096
)
```

```
s_floatField2 = hiCreateFloatField(
?name 'lay1t
?prompt "Thickness (um) "
?enabled 'nil
?value192.5
)
```

```
s_floatField3 = hiCreateFloatField(
?name 'lay2r
?prompt "Layer2:      Rho "
?enabled 'nil
```

```
?value3.0993
```

```
)
```

```
s_floatField4 = hiCreateFloatField(
```

```
?name 'lay2t
```

```
?prompt "Thickness (um) "
```

```
?enabled 'nil
```

```
?value6.8
```

```
)
```

```
s_floatField5 = hiCreateFloatField(
```

```
?name 'lay3r
```

```
?prompt "Layer3:      Rho "
```

```
?enabled 'nil
```

```
?value.17621
```

```
)
```

```
s_floatField6 = hiCreateFloatField(
```

```
?name'lay3t
```

```
?prompt "Thickness (um) "
```

```
?enabled 'nil
```

```
?value 0.7
```

```
)
```

```
(hiCreateAppForm
?name      'sModelfitSetup
?formTitle "Parameter Extraction Setup"
?callback  "(sncExec)"
?fields    (list (list pject_name 10:10 300:24 150)
;;(list custom_model 310:8 200:24 10)
(list data_select 10:40 200:24 150)
(list data_saved 20:65 300:24 140)
(list profile_select 10:100 200:24 150)
(list profile_name 20:125 300:24 140)
;(list s_label60:170 200:24)
(list num_layers10:160 200:24 150)
(list s_floatField1 20:200 220:24 115)
(list s_floatField2 250:200 220:24 100)
(list s_floatField3 20:230 220:24 115)
(list s_floatField4 250:230 220:24 100)
(list s_floatField5 20:260 220:24 115)
(list s_floatField6 250:260 220:24 100)
)
)
```

```
hiDisplayForm(sModelfitSetup)
)

(defun sncCalibGUI ()

  pject_name      = (hiCreateStringField
  ?name'pject_name
  ?prompt "Choose a directory:"
  ?value "substrate1"
  )

  profile_name= (hiCreateStringField
  ?name'profile_name
  ?prompt "Profile Name:"
  ?value "profile1"
  )

  (hiCreateAppForm
  ?name      'sCalibSetup
  ?formTitle "Substrate Calibration Setup"
  ?callback  "(sncRunCalib)"
  ?buttonLayout 'OKCancelDef
  ?fields    (list pject_name profile_name)
```

```
)

hiDisplayForm(sCalibSetup)
)

(defun sncCharacterizeSubstrateGUI ()

  calibrate= (hiCreateButton
    ?name'calibrate
    ?buttonText "Calibrate EPIC"
    ?callback "(sncCalibGUI)"
  )

  modelfit= (hiCreateButton
    ?name'modelfit
    ?buttonText "Generate Model Parameters"
    ?callback "(sncModelfitGUI)"
  )

  (hiCreateAppForm
    ?name      'sCharacterizeTool
    ?formTitle "Substrate Characterization Tool"
```

```
?buttonLayout 'OKCancel  
?fields      (list calibrate modelfit)  
)  
  
hiDisplayForm(sCharacterizeTool)  
)
```

## Appendix D – Modifications to the Calibration Routine

This appendix lists a few changes that were made to the original calibration routine which improve functionality and performance.

- Hard coded parameters were moved to the input file which now contains all of the data which is subject to change between calibration runs. These items include: die thickness, bulk resistivity, the number of layers in the substrate, the initial resistivity and thickness for each layer, the contacts used for input  $Z_{11}$  measurements and the measured  $Z_{11}$  values. For constrained versions of the calibration routine, the constraining values are also contained in the input file.
- Fixed length arrays, which relate to the LMA, are now assigned dynamically. This allows a single build to handle any number of substrate layers and any number of measurements.
- The interface with EPIC was adjusted to accommodate the other changes made to the calibration code.
- Several versions of the calibration routine were created which provide different options. These include: a version that implements constrained optimization, versions which allow certain parameters to stay fixed at a user defined

value, and a version which uses the original implementation but incorporates the changes listed above.

